

Force-induced desorption of copolymeric comb polymers

E J Janse van Rensburg*, C E Soteros‡ & S G Whittington†

* Department of Mathematics and Statistics, York University, Toronto, M3J 1P3, Canada

‡ Department of Mathematics and Statistics, University of Saskatchewan, Saskatoon, S7N 5E6, Canada

† Department of Chemistry, University of Toronto, Toronto, M5S 3H6, Canada

E-mail: *rensburg@yorku.ca, ‡soteros@math.usask.ca, †stuart.whittington@utoronto.ca

5 December 2023

Abstract. We investigate a lattice model of comb copolymers that can adsorb at a surface and that are subject to a force causing desorption. The teeth and the backbone of the comb are chemically distinct and can interact differently with the surface. That is, the strength of the surface interaction can be different for the monomers in the teeth and in the backbone. We consider several cases including (i) the uniform case where the number of teeth is fixed and the lengths of the branches in the backbone and the lengths of the teeth are all identical, (ii) the case where the teeth are short compared to the branches in the backbone, (iii) the situation where the teeth are long compared to the backbone, and (iv) the case where the number of teeth approaches infinity. We determine the free energies in the thermodynamic limit and discuss the nature of the phase diagrams of the model.

PACS numbers: 82.35.Lr, 82.35.Gh, 61.25.Hq

AMS classification scheme numbers: 82B41, 82B80, 65C05

Keywords: Self-avoiding walk, copolymer combs, phase diagram

1. Introduction

The introduction of experimental techniques such as atomic force microscopy [10, 40] has made possible the micro-manipulation of individual polymer molecules and allowed the investigation of how individual polymer molecules respond to applied forces. This has led to renewed interest in the theoretical treatment of this topic [1, 12, 13, 19]. For a review, see for instance [30].

A particular case that has attracted attention is when the polymer is adsorbed at a surface and is desorbed by the action of the force [5, 18, 20, 24, 25, 28]. Several different models have been investigated [30] but we shall concentrate here on interacting models of self-avoiding walks [15, 27] and related systems. For other related work, see [2, 32, 33].

Polymer adsorption is important in steric stabilization of colloids [29] and linear polymers terminally attached to a surface can be used as steric stabilizers. Other polymer architectures such as stars and brushes have been used for this purpose. Block copolymers are also useful for steric stabilization, where one block adsorbs on the surface and the other extends into the solution. In particular, comb polymers with the backbone and teeth having different chemical composition (see figure 1) have been investigated experimentally [39]. These have several parameters that can be varied, including the length and spacing of the teeth of the comb and the chemical compositions of the teeth and backbone.

There are a few studies of the self-avoiding walk model of homopolymeric star polymers, adsorbed at a surface and subject to a desorbing force [3, 4, 21, 22]. For an investigation of the same situation for some models of homopolymeric branched polymers, including uniform combs, see reference [22]. Even fewer papers [17, 23] have appeared on self-avoiding walk models of copolymers adsorbed at a surface and subject to a force. Linear AB diblock copolymers and ABA triblock copolymers have been studied where the A and B monomers interact differently with the surface [17]. One end monomer, *ie* a vertex of degree 1, of the copolymer is grafted to the surface and the force is applied either at the opposite end (the other degree 1 vertex) of the block copolymer or at the central vertex. Copolymeric stars have also been considered [23]. Think of a multi-arm star with some arms (or branches) of type A and the remaining arms of type B . A vertex of degree 1 is fixed in the surface (say of an A -arm) and the force is applied either at a degree 1 vertex of type A or B , or at the central vertex. In each case the general form of the phase diagram has been established [23].

In this paper we explore the problem of copolymeric comb polymers where the backbone and the teeth have different chemical composition; see figure 1 for a schematic diagram. This is a generalization and extension of a treatment of a self-avoiding walk model of homopolymeric combs, pulled from a surface at which they adsorb, studied in [22]. There it was shown that there is a critical force where the comb is pulled from an adsorbed phase into a ballistic phase. An applied force at the terminal end of the backbone may be strong enough to pull off both the last segment of the backbone and the last tooth. In this case it desorbs the entire comb. There is also the possibility that the force is strong enough to pull off the last segment (or branch) of the backbone, but not the last tooth. In this case the teeth remain adsorbed, and the comb only desorbs completely if the strength of the force is increased to also pull off the last tooth.

A lattice model of a copolymeric comb is illustrated in figure 2. The comb is embedded in the cubic lattice \mathbb{Z}^3 (or more generically, in the d -dimensional hypercubic lattice). Attaching the coordinates (x_1, x_2, x_3) to the lattice sites (with each coordinate an integer), the comb in figure 2 is also in the *half-lattice* \mathbb{L}^3 of all lattice sites with $x_3 \geq 0$. The half-lattice has a boundary (hard wall) $x_3 = 0$ that will also be called the *adsorbing surface* or *adsorbing plane*.

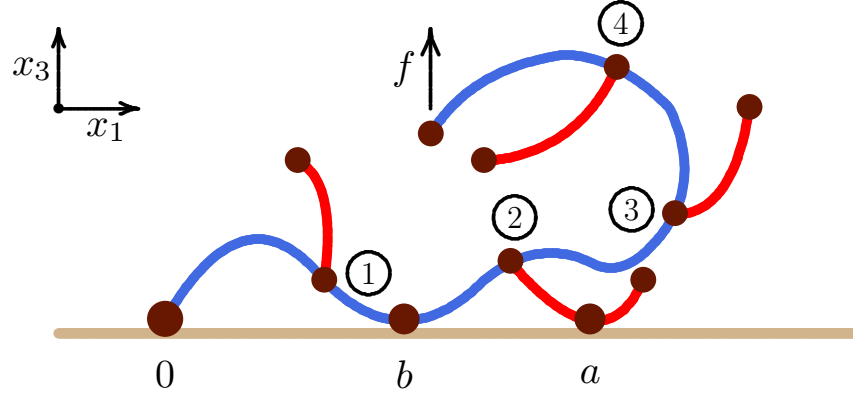


Figure 1. A schematic diagram of a pulled adsorbing comb block copolymer. The comb consists of a backbone (blue) consisting of B -type monomers and t teeth (red) consisting of A -type monomers. An endpoint of the comb's backbone is grafted to the origin on the adsorbing surface $x_3 = 0$, and the other endpoint of its backbone is pulled vertically by a force f . Monomers along the backbone adsorb on the adsorbing surface with activity $b = e^{-\epsilon_B/k_B T}$ where ϵ_B is a binding energy, T is the absolute temperature and k_B is Boltzmann's constant. Monomers in the teeth of the comb similarly adsorb on the adsorbing surface, but with activity $a = e^{-\epsilon_A/k_B T}$ where ϵ_A is a binding energy. Starting from the origin and moving along the backbone, the trivalent vertices (branch points) are labelled $1, 2, \dots, t$ as indicated in circles, where the number of teeth $t = 4$ in this case. The teeth are similarly labelled according to the label of the trivalent vertex from which they emanate. Branches of the backbone are labelled with $1, \dots, t + 1$ so that the branch between the trivalent vertices $i - 1$ and i has label i . We assume that each backbone branch has length m_b and each of the teeth has length m_a .

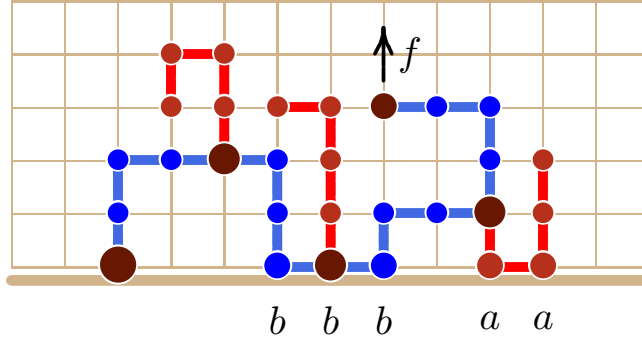


Figure 2. A lattice copolymeric comb. The backbone of the comb adsorbs with activity b , and the teeth with activity a . A vertical force f pulls the comb at its endpoint, while its other endpoint is grafted at the origin. This comb has 3 teeth.

The backbone of the comb in figure 2 is composed of B -monomers, and has length 16 consisting of 4 segments or *branches*, each of length $m_b = 4$. The comb has $t = 3$ teeth composed of A -monomers, each of length $m_a = 3$. The total size of the comb is $(t + 1)m_b + tm_a = 28$. The backbone of the comb makes $v_B = 3$ visits, each of weight b , to the adsorbing plane, and the teeth make $v_A = 2$ visits, each of weight a . The last vertex of the backbone is at a height $h = 3$ above the adsorbing plane. Putting $y = e^{f/k_B T}$, where f is the applied force, k_B is Boltzmann's constant

and T is the absolute temperature, the partition function of the comb is

$$K^{(t)}(m_a, m_b, a, b, y) = \sum_{v_A, v_B, h} k^{(t)}(m_a, m_b, v_A, v_B, h) a^{v_A} b^{v_B} y^h, \quad (1)$$

where $k^{(t)}(m_a, m_b, v_A, v_B, h)$ is the number of combs, with one terminal vertex attached to the surface, with t teeth, each of length m_a , $t + 1$ backbone branches of length m_b , having v_A tooth vertices in the surface and $v_B + 1$ backbone vertices in the surface, and with the other terminal vertex at height h above the surface. The thermodynamic limit of this model can be examined in several cases. In the first instance, putting $m_b = m_a = m$ gives a uniform comb, and taking $m \rightarrow \infty$ (with t fixed) gives a sparsely branched comb with a long backbone and long teeth. Other limits can be taken by taking $m_b \rightarrow \infty$ with m_a fixed, or taking $m_a \rightarrow \infty$ with m_b fixed. There is also the limit $t \rightarrow \infty$, followed by either $m_b \rightarrow \infty$ or $m_a \rightarrow \infty$, or both. We shall investigate some of these limits.

The plan of the paper is as follows. In section 2 we recall some results about self-avoiding walks adsorbing at a surface and subject to a desorbing force, and in the same section we prove some lemmas that we shall need later in the paper.

In section 3 we look at the case of uniform combs where $m_a = m_b = m$ (so that all branches in the backbone and teeth are the same length) and the number of teeth, t , is fixed. We derive expressions for the free energy and give the general features of the phase diagram as slices at constant a , constant b and constant y . In section 4 we examine the situations where the backbone is long compared to the teeth, and where the teeth are long compared to the backbone, still with t fixed. These cases give rise to two limiting cases, one where the comb behaves like a self-avoiding walk and the other where it behaves like a star. In section 5 we examine the infinite t limit, and we close with a short discussion in section 6.

2. Some background results

2.1. Adsorbing and pulled walks

In this section we give a brief account of previous results, concentrating on self-avoiding walks. We shall need some of these results in the following sections where we construct combs from collections of self-avoiding walks and stars. We focus on the simple cubic lattice \mathbb{Z}^3 but some of the results for self-avoiding walks can be extended to \mathbb{Z}^d for all $d \geq 2$.

Consider self-avoiding walks in \mathbb{Z}^3 where we attach the standard coordinate system (x_1, x_2, x_3) so that lattice vertices have integer coordinates. For an n -edge self-avoiding walk, number the vertices $k = 0, 1, \dots, n$ and write $x_i(k)$ for the i -th coordinate of the k -th vertex. Write c_n for the number of n -edge self-avoiding walks starting at the origin. It is known that the limit

$$\lim_{n \rightarrow \infty} \frac{1}{n} \log c_n = \inf_{n > 0} \frac{1}{n} \log c_n \equiv \log \mu_3 \quad (2)$$

exists [6] and μ_3 is called the *growth constant* of the lattice (while $\kappa_3 = \log \mu_3$ is the *connective constant* of the lattice).

An n -edge self-avoiding walk is *unfolded in the x_i -direction* (or *x_i -unfolded*) if $x_i(0) < x_i(k) \leq x_i(n)$ for all $1 \leq k \leq n$. It has x_i -span equal to $x_i(n) - x_i(0)$. We shall write c_n^\dagger (since the count is independent of i) for the number of these unfolded walks. It is known [8] that

$$c_n^\dagger = \mu_3^{n+O(\sqrt{n})}. \quad (3)$$

In general we use the superscript \dagger to show that a walk is unfolded and $\dagger[i]$ when we need to emphasise that the unfolding is in the i -th direction.

If the walk is *doubly unfolded*, then it is unfolded in one direction and then unfolded again in a second direction, and we use the superscript \ddagger , or $\ddagger[ij]$ if we need to specify the two unfolding directions.

If a self-avoiding walk satisfies the constraint that $x_3(k) \geq 0$ for $0 \leq k \leq n$ then the walk is a *positive walk* (see figure 3). A positive walk can also be unfolded. If we write c_n^+ for the number of positive walks with n edges, and $c_n^{+\dagger[3]}$ for the number of positive walks with n edges, unfolded in the x_3 -direction, then $\lim_{n \rightarrow \infty} \frac{1}{n} \log c_n^+ = \lim_{n \rightarrow \infty} \frac{1}{n} \log c_n^{+\dagger[3]} = \log \mu_3$ [8, 36].

If a positive walk is constrained to start and end in the plane $x_3 = 0$, then it is a *loop*. If we write ℓ_n for the number of loops with n edges, and $\ell_n^{\dagger[1]}$ for the number of loops, unfolded in the x_1 -direction, with n edges, then $\lim_{n \rightarrow \infty} \frac{1}{n} \log \ell_n = \lim_{n \rightarrow \infty} \frac{1}{n} \log \ell_n^{\dagger[1]} = \log \mu_3$ [8, 36]. By symmetry, the same result holds for loops unfolded in the x_2 -direction.

All these results are also valid in the square lattice (or, more generally, in the hypercubic lattices).

Let $c_n^+(v, h)$ be the number of n -edge positive walks, starting at the origin, having $v+1$ vertices in the plane $x_3 = 0$ and with $x_3(n) = h$. We say that the walk has v *visits* and that the *height* of the last vertex is h . Define the partition function $C_n^+(a, y) = \sum_{v, h} c_n^+(v, h) a^v y^h$. The limit

$$\lim_{n \rightarrow \infty} \frac{1}{n} \log \sum_{v, h} c_n^+(v, h) a^v y^h = \lim_{n \rightarrow \infty} \frac{1}{n} \log C_n^+(a, y) \equiv \psi(a, y) \quad (4)$$

exists for all a and y [18] and $\psi(a, y)$ is the *free energy* of the model. (We use lower case letters for counts, upper case letters for partition functions, and Greek letters for free energies.) Here $a = \exp[-\epsilon/k_B T]$ and $y = \exp[f/k_B T]$ where ϵ is the energy associated with a vertex in the surface, k_B is Boltzmann's constant, T is the absolute temperature and f is the force normal to the surface (measured in energy units).

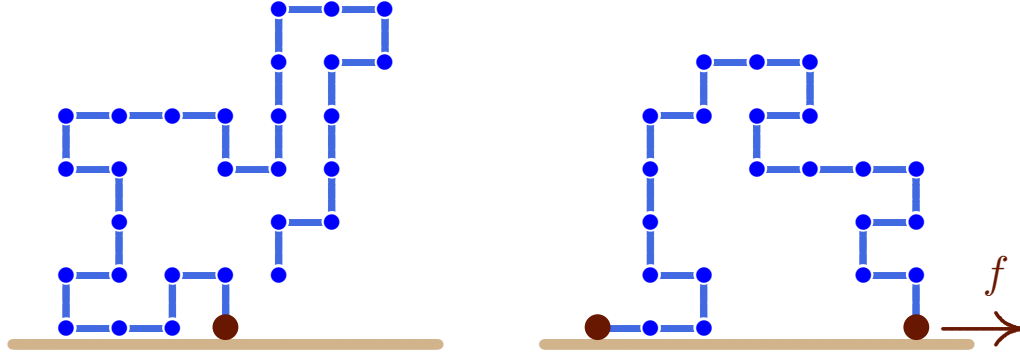


Figure 3. (Left) A positive walk in the half-space $x_3 \geq 0$. (Right) An x_1 -unfolded loop in the half-space $x_3 \geq 0$. This loop is pulled at its last vertex by a horizontal force f parallel to the hard wall (boundary of the half-space).

We can turn off the force by setting $y = 1$ and we then have the pure adsorption problem where $\psi(a, 1) \equiv \kappa(a)$. The free energy $\kappa(a)$ is a convex function of $\log a$ [7] and is therefore continuous.

There exists a critical value of a , $a_c > 1$, such that $\kappa(a) = \log \mu_3$ when $a \leq a_c$ and $\kappa(a) > \log \mu_3$ when $a > a_c$ [7, 14, 26].

If we write $\ell_n(v)$ for the number of loops with n edges and $v + 1$ vertices in the plane $x_3 = 0$ then [7]

$$\lim_{n \rightarrow \infty} \frac{1}{n} \log \sum_v \ell_n(v) a^v = \lim_{n \rightarrow \infty} \frac{1}{n} \log L_n(a, 1) = \kappa(a). \quad (5)$$

We say that $\ell_n(v)$ is the number of adsorbing loops with n edges and v visits, and $L_n(a, 1)$ is the partition function for loops with no applied force. The free energy $\kappa(a)$ is unchanged when the walks or loops are unfolded, or even doubly unfolded [7], or when the endpoints of loops are restricted to a line (for example, to the x_1 -axis), see, for example, reference [15, section 9.1]. Restricting any of these walks or loops to a quarter space (for example $x_i \geq 0$ for $i \in \{1, 2\}$) also leaves $\kappa(a)$ unchanged, even if endpoints are restricted to be located in a line. For example, if adsorbing loops are unfolded in the x_1 -direction (see figure 3) their partition function is $L_n^{\dagger[1]}(a, 1)$ and their free energy is also equal to $\kappa(a)$ [7]. The free energy is unchanged for the subset of these loops restricted to the quarter space $x_2, x_3 \geq 0$ and having end points in the x_1 -axis.

We can turn off the interaction between a positive walk and the surface by setting $a = 1$ so that the surface just acts as an impenetrable barrier (or hard wall) and we can then write $\psi(1, y) \equiv \lambda(y)$. $\lambda(y)$ is a convex function of $\log y$ [16], $\lambda(y) = \log \mu_3$ for $y \leq 1$ and $\lambda(y) > \log \mu_3$ for $y > 1$ [1, 12]. This is the free energy of pulled positive walks. If the positive walks are unfolded, or doubly unfolded, in any direction, then the free energy is unchanged. For example, if the pulled walks are unfolded in the x_3 -direction, then the partition function is $C_n^{+\dagger[3]}(1, y)$ and the free energy is $\lambda(y)$ [19].

Pulled positive walks are a special case of walks (not necessarily positive) terminally attached to the origin and then pulled at the other end by a force f in the x_3 direction; we call these x_3 -pulled walks. The partition function for these walks is denoted here by $C_n(y)$ with y being conjugate to the x_3 -span of the walk. $C_n(y) \geq C_n^+(1, y)$ and its limiting free energy is also $\lambda(y) = \psi(1, y)$ for $y \geq 1$. This follows from unfolding arguments that give the string of inequalities

$$C_n^+(1, y) \leq C_n(y) \leq C_n^{\dagger[3]}(y) e^{O(\sqrt{n})} \leq C_n^+(1, y) e^{O(\sqrt{n})} \quad \text{for } y \geq 1. \quad (6)$$

For general values of a and y [18]

$$\psi(a, y) = \max[\kappa(a), \lambda(y)] \quad (7)$$

so $\psi(a, y) = \log \mu_3$ when $a \leq a_c$ and $y \leq 1$. This is the *free phase*. There are phase boundaries in the (a, y) -plane at $a = a_c$ for $y \leq 1$, at $y = 1$ for $a \leq a_c$ and at the solution of $\kappa(a) = \lambda(y)$ for $a \geq a_c$ and $y \geq 1$. The phase diagram has three phases and the phase transition for $y > 1$ and $a > a_c$ between the *adsorbed phase* and the *ballistic phase* is first order [5].

The definitions for positive walks and loops above are all relative to a fixed boundary surface $x_3 = 0$ and a corresponding half-space $x_3 \geq 0$. The same results hold for *negative* walks and loops in the half-space $x_3 \leq 0$. Similarly, the results hold for other choices for the fixed boundary surface $x_i = 0$, $i \in \{1, 2\}$, and we define x_i -positive (negative) walks and loops for these cases. We also refer to x_i -loops as loops oriented in the x_i direction. Also by symmetry, results about x_3 -pulled walks apply equally to x_i -pulled walks $i \in \{1, 2\}$ where y is conjugate to x_i -span.

In some of the constructions that we use later in the paper we shall make extensive use of the properties of loops, and we shall need several new results about loops. If the endpoint of a loop (oriented in the x_3 -direction) is pulled by a force f parallel to the x_1 -direction (see the right panel of figure 3), then it is both *adsorbing and pulled*. We write $\ell_n(v, s)$ for the number of loops of n

edges with v visits and x_1 -span equal to $s = x_1(n) - x_1(0)$ (the distance between its endpoints in the x_1 -direction), then, provided that the Boltzmann factor for adsorbed vertices is $a = 1$ and $y \geq 1$,

$$\lim_{n \rightarrow \infty} \frac{1}{n} \log L_n(1, y) = \lim_{n \rightarrow \infty} \frac{1}{n} \log \sum_{v,s} \ell_n(v, s) y^s = \lambda(y). \quad (8)$$

This is also the case if $L_n(1, y)$ is replaced by the x_i -unfolded loop partition function $L_n^{\dagger[i]}(1, y)$ for $i = 1, 2$, or even for the partition function $L_n^{\dagger[1,2]}(1, y)$ of doubly unfolded loops in the x_1 and x_2 directions. The lemma also applies to these models when the walks are confined to a quarter lattice defined by $x_2, x_3 \geq 0$ and if the endpoints of the loops are restricted to the x_1 -axis and pulled parallel to the x_1 axis. We prove this result for the partition functions $L_n^{\dagger[1]}(1, y)$ and $L_n(1, y)$ in the lemma 1. The proofs for the other models are similar.

Lemma 1. *For loops with no interaction with the surface ($a = 1$) and pulled parallel to the surface (in the x_i -direction, $i \in \{1, 2\}$), the free energy is $\lambda(y)$ for $y \geq 1$. If the loops are unfolded in the x_i -direction they have free energy, $\lambda(y)$, for all $y > 0$.*

Proof: Consider $i = 1$ and $y \geq 1$. Write $L_n(1, y) = \sum_{v,s} \ell_n(v, s) y^s$ for the partition function of loops with n edges, pulled in the x_1 -direction, and write $L_n^{\dagger[1]}(1, y)$ for the partition function of loops, unfolded and pulled in the x_1 -direction. Such loops are examples of x_1 -pulled walks, thus by inclusion, for $y \geq 1$

$$L_n^{\dagger[1]}(1, y) \leq L_n(1, y) \leq C_n(y) = \exp[\psi(1, y)n + o(n)].$$

Consider self-avoiding walks unfolded in the x_1 -direction and subject to a force in the same direction. These are examples of x_1 -pulled x_1 -positive walks. Suppose that their partition function is $C_n^{\dagger[1]}(y)$. Then $C_n^{\dagger[1]}(y) \leq C_n^{\dagger[1]}(1, y)$ by inclusion. Unfolding cannot decrease the distance between the end-points in the unfolding direction so, via equation (3), for $y \geq 1$, $C_n^{\dagger[1]}(1, y) \leq C_n(y) \leq C_n^{\dagger[1]}(y)e^{O(\sqrt{n})}$. Therefore

$$C_n^{\dagger[1]}(y) = \exp[\psi(1, y)n + o(n)].$$

Consider n -edge self-avoiding walks pulled and unfolded in the x_1 -direction, and consider the subset of these walks unfolded in the x_3 -direction. Write $C_n^{\dagger[13]}(y)$ for their partition function. Then

$$C_n^{\dagger[13]}(y) \leq C_n^{\dagger[1]}(y) \leq C_n^{\dagger[13]}(y) \exp[O(\sqrt{n})].$$

Consider the subset of these walks with the *most popular span* in the x_3 -direction.[‡] By concatenating such a walk with most popular span in the x_3 direction and the reverse of such a walk (joined by an additional edge) a loop of length $2n + 1$ edges is obtained, pulled and unfolded in the x_1 -direction.

There are at least $\left(C_n^{\dagger[13]}(y)/(n+1)\right)^2$ such loops obtained by this construction so

$$L_{2n+1}^{\dagger[1]}(1, y) \geq \left(\frac{C_n^{\dagger[13]}(y)}{n+1}\right)^2 = \exp[2\psi(1, y)n + o(n)]$$

Therefore $L_n(1, y) = \exp[\psi(1, y)n + o(n)]$ and $L_n^{\dagger[1]}(1, y) = \exp[\psi(1, y)n + o(n)]$.

For $y < 1$, the lemma is a corollary of lemma 1 and theorem 1 in reference [19]. \square

[‡] The most popular x_3 -span is that value of the span giving a maximal contribution to the partition function. That is, the most popular span refers to an x_3 -span such that the contribution to the partition function $C_n^{\dagger[13]}(y)$ due to walks with that span is at least as large as the contribution due to any other x_3 -span.

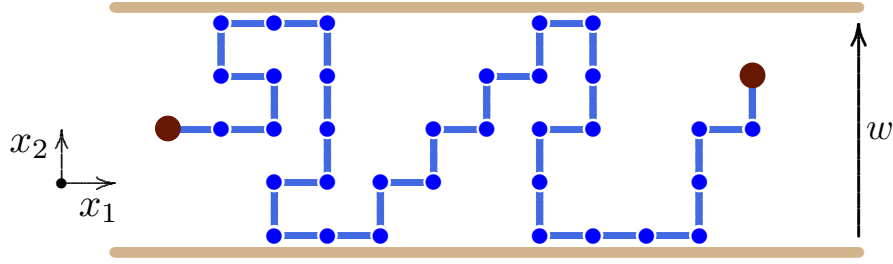


Figure 4. An unfolded walk from the origin in the slab S_w of width w defined by all vertices j with $0 \leq x_2(j) \leq w$. The x_3 direction is normal to the plane of the page.

2.2. Confined walks

In addition to the above results, we shall also need a result on walks confined to *slabs*.

The situation we consider is illustrated in figure 4. A positive walk from the origin in the half space $x_3 \geq 0$ and adsorbing in the $x_3 = 0$ plane is also confined to a slab S_w with boundaries being the two planes $x_2 = 0$ and $x_2 = w$. That is, this walk is adsorbing in the plane $x_3 = 0$ (namely the (x_1, x_2) -plane shown in the figure) and is confined in the slab with $x_3 \geq 0$ between the two planes $x_2 = 0$ and $x_2 = w$ normal to the x_2 -direction and a distance w apart (these two planes project to the horizontal lines bounding the slab in figure 4). Denote the number of these walks of length n by $c_n^{(w)}$. Using the methods in references [9, 35, 37, 38] it can be shown that the limit

$$\lim_{n \rightarrow \infty} \frac{1}{n} \log c_n^{(w)} = \log \mu^{(w)} \quad (9)$$

exists, and that $\mu^{(w)} < \mu^{(w+1)} < \mu_3$ and $\lim_{w \rightarrow \infty} \mu^{(w)} = \mu_3$.

We extend these results to walks adsorbing in the $x_3 = 0$ plane below. The partition function of these walks is then

$$C_n^{(w)}(a) = \sum_v c_n^{(w)}(v) a^v, \quad (10)$$

where $c_n^{(w)}(v)$ is the number of walks with v vertices in the plane $x_3 = 0$ (apart from the origin), and confined to the slab S_w .

Next, consider the walks in $C_n^{(w)}(a)$ which are unfolded in the x_1 -direction (that is, $x_1(0) < x_1(j) \leq x_1(n)$ for $1 \leq j \leq n$ and $0 \leq x_2(k) \leq w$ for $0 \leq k \leq n$). Denote the number of these unfolded walks of length n in S_w having v vertices (apart from the origin) in the adsorbing plane $x_3 = 0$ by $c_n^{\dagger[1],(w)}(v)$, and the corresponding partition function by $C_n^{\dagger[1],(w)}(a)$.

In addition, let $L_n^{\ddagger[1],(w)}(a)$ denote the partition function of walks contributing to $C_n^{\dagger[1],(w)}(a)$ which are also loops *with both endpoints in the x_1 -axis*. That is, x_1 -unfolded walks in the slab with $x_j(0) = x_j(n) = 0, j = 2, 3$. In this case, the double dagger superscript does not denote double unfolding but instead denotes that the endpoints of the loops are restricted to the surface $x_3 = 0$ and also to the line $x_2 = x_3 = 0$ (namely the x_1 -axis). This subset of unfolded loops will be used in constructions later in the paper.

We have the following lemma.

Lemma 2. *The limit $\lim_{n \rightarrow \infty} \frac{1}{n} \log C_n^{(w)}(a) = \kappa^{(w)}(a)$ exists. Moreover, $\kappa^{(w-1)}(a) \leq \kappa^{(w)}(a) < \kappa(a)$, $\kappa^{(w)}(1) = \log \mu^{(w)}$ and $\lim_{w \rightarrow \infty} \kappa^{(w)}(a) = \kappa(a)$.*

The same results hold if the walks in S_w are restricted to the quarter space $x_1, x_3 \geq 0$ and/or restricted to loops or x_1 -unfolded loops with or without the endpoints restricted to the x_1 -axis.

Proof: Unfolded loops with both endpoints in the x_1 -axis contributing to the partition function $L_n^{\dagger[1],(w)}(a)$ can be concatenated with unfolded loops in the partition function $L_m^{\dagger[1],(w)}(a)$ by placing the first vertex of the second loop on the last vertex of the first loop. This shows that

$$L_m^{\dagger[1],(w)}(a) L_n^{\dagger[1],(w)}(a) \leq L_{m+n}^{\dagger[1],(w)}(a)$$

and this establishes the existence of the limit $\lim_{n \rightarrow \infty} n^{-1} \log L_n^{\dagger[1],(w)}(a)$.

By inclusion, $L_n^{\dagger[1],(w)}(a) \leq L_n^{\dagger[1],(w)}(a) \leq L_n^{(w)}(a) \leq C_n^{(w)}(a)$. Similarly, $C_n^{\dagger[1],(w)}(a)$ and the partition functions for walks or loops in S_w and restricted to the quarter space $x_1, x_3 \geq 0$ fit between these two extremes.

Consider the subset of walks from the origin, confined to S_w , unfolded in the x_1 -direction, with partition function $C_n^{\dagger[1],(w)}(a)$. There is a subset of these walks with most popular (x_2, x_3) -coordinates of their end-point. Such walks can be concatenated with a reverse of such a walk (and an additional edge in the x_1 -direction), to form a loop with endpoints in the x_1 -axis. This gives the bound

$$\left(C_n^{\dagger[1],(w)}(a)\right)^2 \leq \max(1, a) (n+1)^2 (w+1)^2 L_{2n+1}^{\dagger[1],(w)}(a).$$

Since $L_n^{\dagger[1],(w)}(a) \leq C_n^{\dagger[1],(w)}(a)$ and $C_n^{\dagger[1],(w)}(a) \leq C_n^{(w)}(a) \leq C_n^{\dagger[1],(w)}(a) e^{O(\sqrt{n})}$ this completes the proof that the limits

$$\lim_{n \rightarrow \infty} \frac{1}{n} \log L_n^{\dagger[1],(w)}(a) = \lim_{n \rightarrow \infty} \frac{1}{n} \log C_n^{(w)}(a) = \kappa^{(w)}(a)$$

exist.

Setting $a = 1$ turns off the interaction with the $x_3 = 0$ plane, it follows that $\kappa^{(w)}(1) = \log \mu^{(w)}$. It follows by inclusion that $\kappa^{(w-1)}(a) \leq \kappa^{(w)}(a)$.

Since any subwalk with x_2 -span greater than w cannot occur as a subwalk of any walk in the slab S_w , it follows from the pattern theorem for adsorbing half-space walks (see [15, section 7.2]) that $\lim_{n \rightarrow \infty} \frac{1}{n} \log C_n^{(w)}(a) = \kappa^{(w)}(a) < \kappa(a)$.

To prove that $\lim_{w \rightarrow \infty} \kappa^{(w)}(a) = \kappa(a)$, consider, $L_m^{\dagger[1]}(a)$, the partition function for unconfined x_1 -unfolded loops with end points in the x_1 -axis. Its limiting free energy is $\kappa(a)$. Thus for any $\epsilon > 0$ there exists $N = N(\epsilon)$ such that $\frac{1}{m} \log L_m^{\dagger[1]}(a) > \kappa(a) - \epsilon$ for $m \geq N$. These loops will fit into a slab with $w > m$. Fix $w > m \geq N$ and then put $n = mp + q$ with $n \geq N$, non-negative integers p and q , and $0 \leq q < m$. By concatenating p unfolded loops of size m and a final loop of size q ,

$$\frac{pm}{pm+q} (\kappa(a) - \epsilon) \leq \frac{1}{pm+q} p \log L_m^{\dagger[1]}(a) + \log L_q^{\dagger[1]}(a) \leq \frac{1}{n} \log C_n^{(w)}(a).$$

Take $n \rightarrow \infty$ by taking $p \rightarrow \infty$ to obtain $\kappa(a) - \epsilon \leq \kappa^{(w)}(a)$. This completes the proof. \square

3. Uniform combs

3.1. Bounds on the free energy of uniform combs

In this section we are concerned with uniform combs. See figure 2 for a sketch. A comb can be thought of as a self-avoiding walk making up the backbone of the comb, with t teeth attached at regular intervals along the backbone. The teeth are also self-avoiding walks, and the teeth and backbone are mutually avoiding. The comb is placed in the half lattice \mathbb{L}^3 which is that part of the cubic lattice with non-negative x_3 coordinates. The first vertex of the backbone of the comb is grafted at the origin, and all other vertices are in \mathbb{L}^3 .

A comb with t teeth has t vertices of degree 3 and $t + 2$ vertices of degree 1. The number of edges in each subwalk between two adjacent vertices of degree 3 and between the end vertices of degree 3 and the initial and terminal vertices of degree 1 is m_b . The number of edges in each tooth is m_a . The total number of edges in the comb is $n = (t + 1)m_b + tm_a$.

In the uniform case we take $m_a = m_b = m$ so that $n = (2t + 1)m$. In this section we consider t -combs where the number of teeth $t \geq 1$ is a fixed integer and define

$$k_n(v_A, v_B, h) = k^{(t)}(n/(2t + 1), n/(2t + 1), v_A, v_B, h) \quad (11)$$

to be the number of uniform t -combs with a total of n edges, having v_A A -visits and v_B B -visits, and with the x_3 -coordinate of the terminal vertex of the backbone equal to h . The corresponding partition function in terms of the general partition function (1) is

$$K_n(a, b, y) = K^{(t)}(n/(2t + 1), n/(2t + 1), a, b, y) = \sum_{v_A, v_B, h} k_n(v_A, v_B, h) a^{v_A} b^{v_B} y^h. \quad (12)$$

In order to prove existence of a unique limiting free energy $\zeta(a, b, y) = \lim_{n \rightarrow \infty} \frac{1}{n} \log K_n(a, b, y)$ in this model, we shall consider the schematic conformations of adsorbed combs shown in figures 5 and 6. The proof proceeds by establishing lower and upper bounds on $K_n(a, b, y)$.

We proceed by first considering x_1 -unfolded adsorbing B -loops and denote their partition function by $L_n^{\dagger[1]}(b)$. In figure 5 we are interested in such loops along the backbone of the comb with x_1 -spans greater than a constant value w , and we denote the partition function of these by $L_n^{\dagger[1]}(>w, b)$. The remaining loops of x_1 -span less than or equal to w have partition function $L_n^{\dagger[1]}(\leq w, b)$. Then it follows that

$$L_n^{\dagger[1]}(b) = L_n^{\dagger[1]}(>w, b) + L_n^{\dagger[1]}(\leq w, b). \quad (13)$$

A corresponding equation arises for the partition functions for subsets of these loops that are restricted further either to $x_2 \geq 0$ and/or to having end points in the x_1 -axis. We need the following lemma in order to find a lower bound on the free energy of uniform combs.

Lemma 3. *For any fixed $w \geq 0$, $\lim_{n \rightarrow \infty} \frac{1}{n} \log L_n^{\dagger[1]}(>w, b) = \lim_{n \rightarrow \infty} \frac{1}{n} \log L_n^{\dagger[1]}(b) = \kappa(b)$. The same result holds for the subsets of these loops with $x_2 \geq 0$ and/or with the endpoints restricted to the x_1 -axis.*

Proof: Take logarithms on the left hand side of equation (13), divide by n , and let $n \rightarrow \infty$. This gives for this case (and for the other restrictions considered)

$$\kappa(b) = \lim_{n \rightarrow \infty} \frac{1}{n} \log L_n^{\dagger[1]}(b) = \lim_{n \rightarrow \infty} \frac{1}{n} \log \left(L_n^{\dagger[1]}(>w, b) + L_n^{\dagger[1]}(\leq w, b) \right).$$

The walks contributing to $L_n^{\dagger[1]}(\leq w, b)$ correspond to subsets of walks that fit in the slab of width w , S_w , as in figure 4 except now the restricting planes are constant x_1 planes instead of constant

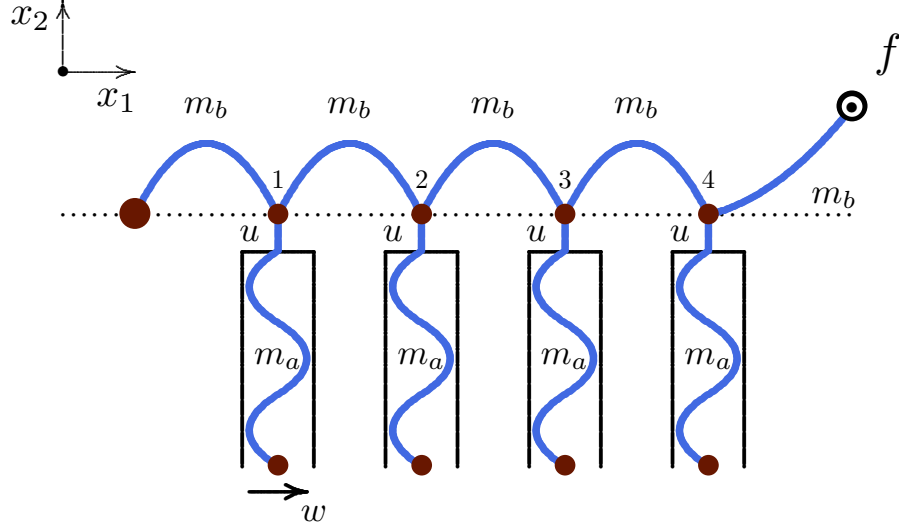


Figure 5. Top view schematic projected onto the x_1x_2 -plane of an adsorbed comb in the half-space $x_3 \geq 0$ grafted at the origin (on the left) and pulled by a vertical force at its endpoint (on the right) from the adsorbing plane. The backbone consists of unfolded loops with endpoints in the x_1 -axis (dotted line) in the half-space $x_2 \geq 0$. The teeth are confined in slabs of width w normal to the x_1 -axis in the half-space $x_2 < 0$.

x_2 planes. By symmetry, the results of lemma 2 also hold for walks in S_w (or with the additional restriction $x_2 \geq 0$). It is thus a corollary of lemma 2 that

$$\limsup_{n \rightarrow \infty} \frac{1}{n} \log L_n^{\dagger[1]}(\leq w, b) \leq \max_{v \leq w} \kappa^{(v)}(b) < \kappa(b).$$

Existence of the limits above then implies that $\lim_{n \rightarrow \infty} \frac{1}{n} \log L_n^{\dagger[1]}(> w, b) = \kappa(b)$. \square

Next, consider figure 6. On the left hand side is a negative x_1 -loop (that is, a loop oriented in the x_1 direction in the half-space $x_1 \leq 0$). It is x_3 -unfolded and pulled by a force in the x_3 -direction. These loops have the same partition function and free energy, $\lambda(y)$ for $y > 0$, as the unfolded loops of Lemma 1. Suppose that the length of the loop is m_b . Then there is a most popular (vertical) distance or *height* between its endpoints, denoted by h_y as in the figure (this is a function of the pulling force $f = k_B T \log y$ and of the length m_b). The number of unfolded loops of length m_b and height h_y is denoted by $\ell_{m_b}^{\dagger[3]}(h)$, and it follows that

$$[\ell_{m_b}^{\dagger[3]}(h_y) y^{h_y}] \leq \sum_{h=0}^{m_b} \ell_{m_b}^{\dagger[3]}(h) y^h \leq (m_b + 1) [\ell_{m_b}^{\dagger[3]}(h_y) y^{h_y}]. \quad (14)$$

Since, by Lemma 1, the free energy of these pulled unfolded loops exists and is equal to $\lambda(y)$, this shows that

$$\lim_{m_b \rightarrow \infty} \frac{1}{m_b} \log [\ell_{m_b}^{\dagger[3]}(h_y) y^{h_y}] = \lambda(y). \quad (15)$$

It is the case that h_y is not bounded, but grows with m_b . This is shown in the next lemma.

Lemma 4. $\liminf_{m_b \rightarrow \infty} h_y = \infty$ for all $y > 0$.

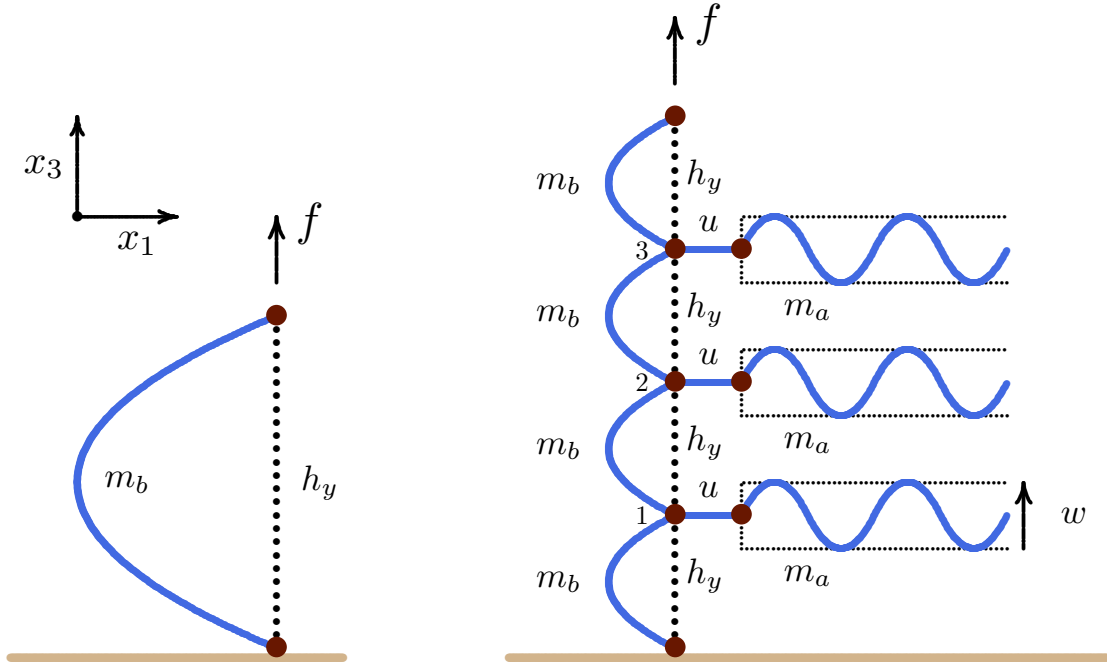


Figure 6. (Left) A schematic drawing of a pulled unfolded loop. The loop is oriented in the half-space $x_1 \leq 0$ and its endpoints are in the plane $x_1 = 0$. A force f is applied in the vertical direction. If the length of the loop is m_b , then there is a most popular vertical separation (or height) h_y between its endpoints. This most popular height is a function of both m_b and y . (Right) Constructing a pulled comb by combining pulled loops with teeth confined to horizontal slits or slabs of (constant) height w . In this case, each loop has length m_b and height h_y (the most popular height at an applied force f). Each tooth has length m_a and is joined to the backbone by a u horizontal edges.

Proof: Suppose that there exists a $w \geq 0$ such that $h_y < w$ for all $m_b \geq 0$. Then $\ell_{m_b}^{\dagger[3]}(h_y) \leq c_{m_b}^{(w)}$ (that is, each loop of length m_b and height h_y is also a self-avoiding walk confined in a slab of width w , bounded by the planes $x_3 = 0$ and $x_3 = w$). Taking logarithms, dividing by m_b and then taking $m_b \rightarrow \infty$ gives via equation (9), for $y > 0$,

$$\lambda(y) = \lim_{m_b \rightarrow \infty} \frac{1}{m_b} \log[\ell_{m_b}^{\dagger[3]}(h_y) y^{h_y}] \leq \lim_{m_b \rightarrow \infty} \frac{1}{m_b} \log[c_{m_b}^{(w)} (\max\{1, y\})^w] = \log \mu^{(w)} < \log \mu_3.$$

This is a contradiction (since $\lambda(y) \geq \log \mu_3$), and thus h_y is not bounded. Since the limit on the left exists, this is valid if the limits are taken along any subsequence, with the result that h_y is unbounded along any subsequence. Thus, for any $N > 0$ there is an M such that $h_y > N$ for all $m_b > M$. \square

Theorem 1. When $y \geq 1$ the free energy for uniform t -combs $\zeta(a, b, y) = \lim_{n \rightarrow \infty} \frac{1}{n} \log K_n(a, b, y)$ is given by

$$\zeta(a, b, y) = \max \left[\frac{t}{2t+1} \kappa(a) + \frac{t+1}{2t+1} \kappa(b), \frac{1}{2t+1} \lambda(y) + \frac{t}{2t+1} (\kappa(a) + \kappa(b)), \frac{t+1}{2t+1} \lambda(y) + \frac{t}{2t+1} \log \mu_3 \right].$$

Proof:

Lower bound: First establish a lower bound by considering t -combs in conformations shown in figures 5 and 6. We label the trivalent nodes in the combs, starting in the node closest to the origin by 1, 2, ..., t , as shown. A lower bound is constructed by considering three cases, based on the schematic diagrams:

- 1) the height of the pulled vertex is 0 (a special case of figure 5);
- 2) the height of trivalent vertex labeled t is 0 and all the vertices in the $(t+1)$ -st branch are out of the surface (see figure 5);
- 3) all vertices of the comb are above the surface except for the origin (see figure 6).

Consider case (1) and figure 5 but with the last (pulled) vertex at height zero. The backbone of the comb is a sequence of t loops unfolded in the x_1 -direction, each of length m_b and confined to the sublattice $x_2 \geq 0$ and $x_3 \geq 0$, with endpoints in the x_1 -axis. The last segment along the backbone is also assumed to be an unfolded loop with endpoints in the x_1 -axis.

Next, assume that the x_1 -span of each loop along the backbone exceeds w . We simplify the presentation by denoting the partition function for each of these loops by $L_n^{\dagger[1]}(>w, b)$ (this includes the restrictions that $x_2 \geq 0$ and the loop endpoints are in the x_1 -axis). Thus by lemma 3 their limiting free energies are $\kappa(b)$.

The teeth in figure 5 are quarantined in slabs of width w (bounded by constant x_1 planes) in the sublattice $x_2 < 0$ and $x_3 \geq 0$, each of length m_a , and interacting with the x_3 -plane. Each tooth is attached to the backbone by a sequence of u edges in the x_2 direction, and one may assume that $u = 1$. By symmetry, these walks have the same partition function as the quarter space walks of lemma 2. For simplicity, we denote that partition function here by $C_{m_a-u}^{(w)}(a)$ (this includes the quarter space restriction). By lemma 2 its limiting free energy is $\kappa^{(w)}(a)$.

Thus, the comb is now put together by assuming each tooth is quarantined in a slab of width fixed at w , and the loops along the backbones have x_1 -spans exceeding w . This shows that for case (1) above,

$$K^{(t)}(m_a, m_b, a, b, y) \geq \left[L_{m_b}^{\dagger[1]}(>w, b) \right]^t \left[L_{m_b}^{\dagger[1]}(b) \right]^1 \left[C_{m_a-u}^{(w)}(a) \right]^t. \quad (16)$$

Next, put $m_a = m_b = m$, take logarithms, divide by $(2t+1)m$, and then take $m \rightarrow \infty$. By lemmas 2 and 3 and equation (7),

$$\liminf_{m \rightarrow \infty} \frac{1}{(2t+1)m} \log K^{(t)}(m, m, a, b, y) \geq \frac{1}{(2t+1)} (t\kappa(b) + \kappa(b) + t\kappa^{(w)}(a)). \quad (17)$$

Since w is arbitrary, one may take $w \rightarrow \infty$ on the right hand side. By lemma 2 $\kappa^{(w)}(a) \rightarrow \kappa(a)$. This gives the lower bound $\frac{t}{2t+1}\kappa(a) + \frac{t+1}{2t+1}\kappa(b)$ from case (1).

Case (2) is treated in the same way, except that the last segment of the backbone is anchored by the t -th trivalent vertex to the adsorbing plane $x_3 = 0$ but is otherwise disjoint from it, and is pulled in its endpoint. This gives the lower bound

$$\liminf_{m \rightarrow \infty} \frac{1}{(2t+1)m} \log K^{(t)}(m, m, a, b, y) \geq \frac{1}{2t+1} (t\kappa(b) + \lambda(y) + t\kappa^{(w)}(a)). \quad (18)$$

Taking $w \rightarrow \infty$ gives the lower bound $\frac{1}{2t+1}\lambda(y) + \frac{t}{2t+1}(\kappa(a) + \kappa(b))$ from case (2).

Consider case (3) next. The proof is again similar to that of case (1), but now loops are stacked in the x_3 -direction as shown in figure 6. Let $y > 0$, fix m_b and choose $w < h_y$, with h_y as defined before equation (14). Put $u = 1$. Then

$$K^{(t)}(m_a, m_b, a, b, y) \geq \left[\ell_{m_b}^{\dagger[3]}(h_y) y^{h_y} \right]^{t+1} \left[C_{m_a-u}^{\dagger[1],(w)} \right]^t. \quad (19)$$

Next, put $m_a = m_b = m$, take logarithms, divide by $(2t+1)m$, and then take $m \rightarrow \infty$. By equation (15) and lemma 2,

$$\liminf_{m \rightarrow \infty} \frac{1}{(2t+1)m} \log K^{(t)}(m, m, a, b, y) \geq \frac{1}{2t+1} \left((t+1)\lambda(y) + t \log \mu^{(w)} \right). \quad (20)$$

By lemma 4, h_y increases to infinity as $m \rightarrow \infty$, thus $w < h_y$ can be made arbitrarily large. Since $\mu^{(w)} \rightarrow \mu_3$, this completes case (3).

This completes the lower bound.

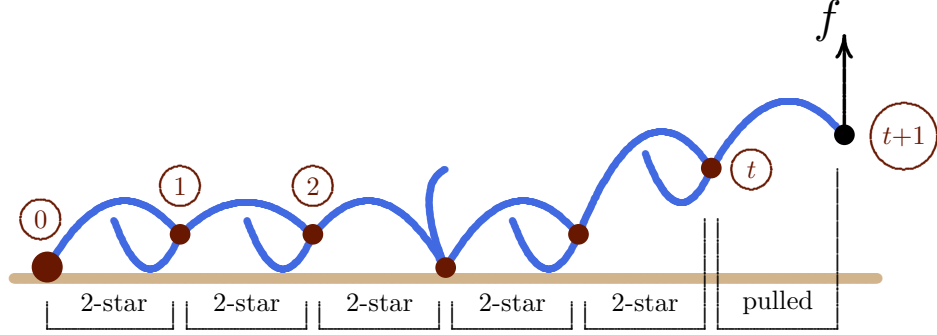


Figure 7. An adsorbing and pulled uniform comb. A force f is pulling at the end of the backbone, desorbing the comb from the surface. Cutting the comb in its trivalent nodes gives a sequence of copolymeric 2-stars and a final branch where the comb is pulled. The trivalent nodes of the comb are labelled starting at the origin by $0, 1, \dots, t, t+1$.

Upper bound:

The case $y \geq 1$: The bound is constructed by viewing the comb as composed of a sequence of copolymer 2-stars, followed by a final pulled branch on the backbone as shown schematically in figure 7. The pulling force f is transmitted along the backbone to the origin, or along the backbone via an absorbed trivalent vertex or a tooth, or an adsorbed branch along the backbone, into the adsorbing plane.

We construct an upper bound by considering the 2-stars to be independent of each other, and bound each from above.

As before, assume that $K^{(t)}(m_a, m_b, a, b, y)$ is the partition function of the comb, where the backbone branches have lengths m_b , the teeth have lengths m_a , and (a, b, y) are the parameters as defined before.

Next, consider one of the 2-stars along the comb (as shown in figure 7). A schematic diagram of such a 2-star is shown in figure 8. The 2-star has arms of lengths equal to m_a and m_b . Each arm is partitioned into a part from the central trivalent node (with label denoted by i in figure 8 and preceded by the trivalent node $i_0 = i - 1$) to its *first visit* in the adsorbing surface, and then a remaining part. The remaining part intersects the adsorbing surface, and those visits are weighted as shown.

The trivalent node $i_0 = i - 1$ in figure 8 is the central node of the preceding 2-star, and it has height h_0 above the adsorbing plane. h_0 is bounded by $0 \leq h_0 \leq (t+1)m_b = H$. The trivalent node i in figure 8 has height h above the adsorbing surface. Clearly, $0 \leq h \leq H$. The pulling force on the comb is transmitted to i and then passed to the adsorbing plane at the visits a or b , or to the node i_0 . Denote the height of the i -th trivalent node by $h^{(i)}$ and the height of the first vertex

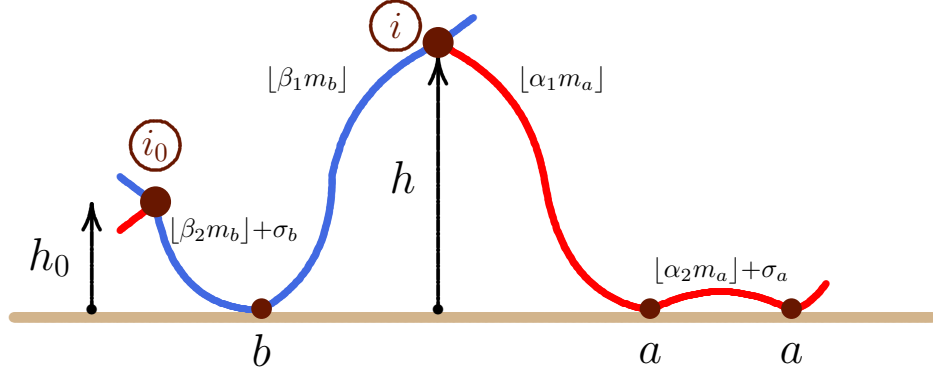


Figure 8. A block copolymeric 2-star in the comb. The trivalent node labelled i is the central node of the star, and $i_0 = i - 1$ is the central node of the preceding 2-star. The arm of the 2-star from i_0 to i has length m_b and is in the backbone of the comb. The pulling force on the comb is transmitted along this arm from i to i_0 . The i -th tooth of the comb is shown on the right, and it is the other arm of the 2-star. It has length m_a and adsorbs in the adsorbing plane with activity a . Vertices in the backbone adsorb with activity b . The lengths of parts of the arms are shown. Here, $\sigma_a, \sigma_b \in \{0, 1\}$.

of the i -th star by $h_0^{(i)} \equiv h^{(i-1)}$. The height of the entire comb is $h^{(t+1)}$ and the height of the final pulled walk is $h^{(t+1)} - h^{(t)}$. Then

$$\sum_{i=1}^{t+1} (h^{(i)} - h^{(i-1)}) = h^{(t+1)} - h^{(0)} = h^{(t+1)}$$

which is the height of the comb. In the partition function of the i -th 2-star the height is defined as $h^{(i)} - h_0^{(i)} = h^{(i)} - h^{(i-1)}$ and this is conjugate to y .

The arm of the 2-star which is also a branch along the backbone of the comb (the blue arm in figure 8) has an *adsorbing part* of length $\lfloor \beta_2 m_b \rfloor + \sigma_b$ and a *pulled part* of length $\lfloor \beta_1 m_b \rfloor$. Here, $\beta_1 + \beta_2 = 1$ and σ_b is a function of (β_1, m_b) such that $\lfloor \beta_1 m_b \rfloor + \lfloor \beta_2 m_b \rfloor + \sigma_b = m_b$. Clearly, $0 \leq \sigma_b \leq 1$.

Similarly, the tooth (the red arm in figure 8) in the 2-star has a pulled part of length $\lfloor \alpha_1 m_a \rfloor$ and an adsorbing part of length $\lfloor \alpha_2 m_a \rfloor + \sigma_a$, where $\alpha_1 + \alpha_2 = 1$ and σ_a is a function of (α_1, m_a) such that $\lfloor \alpha_1 m_a \rfloor + \lfloor \alpha_2 m_a \rfloor + \sigma_a = m_a$. Again, $0 \leq \sigma_a \leq 1$.

Notice that if $\beta_2 > 0$ then $\lfloor \beta_2 m_b \rfloor + \sigma_b \geq h_0$. Similarly, $\lfloor \beta_1 m_b \rfloor \geq h$ and $\lfloor \alpha_1 m_a \rfloor \geq h$.

If $\beta_1 < 1/m_b$, then $h = 0$, and thus $\alpha_1 < 1/m_a$. Similarly, if $\alpha_1 < 1/m_a$, then $h = 0$ and thus $\beta_1 < 1/m_b$. In particular, there is a $0 < \delta < \min(1/m_a, 1/m_b)$ such that $\beta_1 < \delta \Leftrightarrow \alpha_1 < \delta$.

This shows that if $m_a \rightarrow \infty$, or $m_b \rightarrow \infty$, then $\beta_1 = 0 \Leftrightarrow \alpha_1 = 0$.

A similar approach to the above with α_1 and β_1 taking discrete values such that $\alpha_1 m_a$ and $\beta_1 m_b$ are integers can be followed instead.

Proceed by excising the 2-star in figure 8 and considering it in isolation, independent from the rest of the comb. These 2-stars have a fixed end point in one arm at height h_0 above the adsorbing surface, and are pulled in the midpoint by a vertical force, while the arms adsorb with activities a and b .

Copolymer 2-stars terminally attached to the surface and pulled from their midpoint have been studied previously in reference [23]. The 2-star in figure 8 is not terminally attached but rather the

height of the initial vertex is fixed at h_0 where h_0 can range from 0 to $(i-1)m_b \leq (t+1)m_b = H$ in the comb.

Denote by $S_{m_a, m_b}^{\alpha_2 \alpha_1 \beta_1 \beta_2}(h_0; a, b, y)$ the partition function of 2-stars as in figure 8 with $0 \leq h_0 \leq H$ and where y is conjugate to $h - h_0$. If the central vertex of a 2-star is under tension due to the pulling force, then its contribution to the comb partition function is bounded above by

$$\sum_{\alpha_1 m_a=0}^{m_a} \sum_{\beta_1 m_b=0}^{m_b} \sum_{h_0=0}^H S_{m_a, m_b}^{\alpha_2 \alpha_1 \beta_1 \beta_2}(h_0; a, b, y).$$

The summations involving α_1 and β_1 are over all values of α_1 and β_1 such that $\alpha_1 m_a$ and $\beta_1 m_b$ are integers in the sets $\{0, 1, 2, \dots, m_a\}$ and $\{0, 1, 2, \dots, m_b\}$ and these choices fix the values of $\{\alpha_2, \beta_2, \sigma_a, \sigma_b\}$.

Denote the partition function of a pulled and adsorbing self-avoiding walk of length m_b starting in a vertex at height h_0 above the adsorbing surface by $C_{m_b}(h_0; b, y)$. This corresponds to the 2-star partition function with $m_a = 0$. The partition function of the comb is bounded above by the product of the partition functions of the contributing 2-stars and the partition function of the final pulled walk. In the upper bound these contributing factors are treated as independent. Since $y \geq 1$, it follows that

$$K^{(t)}(m_a, m_b, a, b, y) \leq \left[\sum_{\alpha_1 m_a=0}^{m_a} \sum_{\beta_1 m_b=0}^{m_b} \left[\sum_{h_0=0}^H S_{m_a, m_b}^{\alpha_2 \alpha_1 \beta_1 \beta_2}(h_0; a, b, y) \right] \right]^t \sum_{h_0=0}^H C_{m_b}(h_0; b, y) \quad (21)$$

$$\leq [(m_a + 1)(m_b + 1)]^t (H + 1)^{t+1} \left[\max_{\alpha_1, \beta_1, h_0} S_{m_a, m_b}^{\alpha_2 \alpha_1 \beta_1 \beta_2}(h_0; a, b, y) \right]^t \max_{h_0} C_{m_b}(h_0; b, y). \quad (22)$$

The maximum over α_1 and β_1 is over all values of α_1 and β_1 between 0 and 1 and the maxima fix the values of $\{\alpha_2, \beta_2, \sigma_a, \sigma_b\}$.

We continue by putting $m_a = m_b$ and by examining the factors in equation (22).

Claim: Given $\epsilon > 0$, there exists an $M \geq 0$ such that for all $m \geq M$,

$$\frac{1}{m} \log S_{m, m}^{\alpha_2 \alpha_1 \beta_1 \beta_2}(h_0; a, b, y) \leq \begin{cases} \kappa(a) + \kappa(b) + 2\epsilon, & \text{if } \alpha_1 = \beta_1 = 0; \\ \log \mu_3 + \lambda(y) + 2\epsilon, & \text{if } \alpha_2 = \beta_2 = 0; \\ \alpha_2 \kappa(a) + \alpha_1 \log \mu_3 + \beta_1 \lambda(y) + \beta_2 \kappa(b) + 2\epsilon, & \text{otherwise.} \end{cases}$$

Proof of the claim: Each 2-star in figure 8 is partitioned in 4 (possibly empty) subwalks. Ignore intersections between these subwalks.

We now construct bounds on the contributions of the arms of the 2-star to the partition function. Assume first that both arms intersect the adsorbing surface.

In figure 8 the tooth of the 2-star is partitioned into two walks by the first vertex in the adsorbing surface. The second part is an adsorbing walk of length $\lfloor \alpha_2 m_a \rfloor + \sigma_a$, while the first part is a walk of length $\lfloor \alpha_1 m_a \rfloor$ from the trivalent node i to the adsorbing surface.

The other arm of the 2-star is similarly partitioned into an adsorbing walk from the trivalent node i_0 to the adsorbing surface, of length $\lfloor \beta_2 m_b \rfloor + \sigma_b$, and a walk from the trivalent node i to the adsorbing surface, of length $\lfloor \beta_1 m_b \rfloor$ (see figure 8).

Denote the number of self-avoiding walks of length n from a vertex at height h_0 to a vertex at height h by $e_n(h_0, h)$. Note that the partition function introduced in section 2.1 for x_3 -pulled (not necessarily positive) walks $C_n(y) = \sum_h e_n(0, h) y^h = \sum_h e_n(h_0, h) y^{h-h_0}$, independent of h_0 . Also, denote the number of positive self-avoiding walks from the origin making v visits,

including the origin, to the adsorbing surface by $c_n^+(v)$. Denote their partition function by $C_n^+(a) = \sum_v c_n^+(v) a^v = a C_n^+(a, 1)$.

Then counting the walks in figure 8 in terms of $e_n(h_0, h)$ and $c_n^+(v)$ and noting that $y \geq 1$ while $h_0 \geq 0$, the following bound is obtained:

$$\begin{aligned}
S_{m,m}^{\alpha_2\alpha_1\beta_1\beta_2}(h_0; a, b, y) &\leq \left[\sum_h e_{\lfloor \alpha_1 m \rfloor}(0, h) y^{h-h_0} e_{\lfloor \beta_1 m \rfloor}(0, h) \right] \left[\sum_v c_{\lfloor \alpha_2 m \rfloor + \sigma_a}^+(v) a^v \right] \left[\sum_v c_{\lfloor \beta_2 m \rfloor + \sigma_b}^+(v) b^v \right] \\
&\leq c_{\lfloor \alpha_1 m \rfloor} \left[\sum_h e_{\lfloor \beta_1 m \rfloor}(0, h) y^h \right] \left[\sum_v c_{\lfloor \alpha_2 m \rfloor + \sigma_a}^+(v) a^v \right] \left[\sum_v c_{\lfloor \beta_2 m \rfloor + \sigma_b}^+(v) b^v \right] \\
&\leq c_{\lfloor \alpha_1 m \rfloor} C_{\lfloor \beta_1 m \rfloor}(y) C_{\lfloor \alpha_2 m \rfloor + \sigma_a}^+(a) C_{\lfloor \beta_2 m \rfloor + \sigma_b}^+(b). \tag{23}
\end{aligned}$$

Observe that the right hand side of equation (23) is independent of h_0 .

For the three cases when at least one arm of the 2-star does not intersect the adsorbing surface (here, $\alpha_2 = 0$ or $\beta_2 = 0$, or both), it can be verified that the same final upper bound in equation (23) applies.

In addition,

$$\lim_{n \rightarrow \infty} \frac{1}{n} \log C_n^+(a) = \kappa(a) \quad [7] \quad \text{and for } y \geq 1 \quad \lim_{n \rightarrow \infty} \frac{1}{n} \log C_n(y) = \lambda(y) \quad [19].$$

Thus, for an arbitrary and fixed $\epsilon > 0$ there exists an $M > 0$ such that for all $n > M$, $\frac{1}{n} \log C_n^+(a) \leq \kappa(a) + \epsilon$, and $\frac{1}{n} \log C_n(y) \leq \lambda(y) + \epsilon$. Using these in equation (23) shows that there are large, but finite values of $m > M$ (a function of (h_0, a, b)), such that

$$\frac{1}{m} \log S_{m,m}^{\alpha_2\alpha_1\beta_1\beta_2}(h_0; a, b, y) \leq \begin{cases} \kappa(a) + \kappa(b) + 2\epsilon, & \text{if } \alpha_1 = \beta_1 = 0; \\ \lambda(y) + \log \mu_3 + 2\epsilon, & \text{if } \alpha_2 = \beta_2 = 0; \\ \alpha_2 \kappa(a) + \alpha_1 \log \mu_3 + \beta_1 \lambda(y) + \beta_2 \kappa(b) + 2\epsilon, & \text{otherwise.} \end{cases}$$

This completes the proof of the claim. \square

Simplify the cases in the claim by maximizing the expression

$$\alpha_2 \kappa(a) + \alpha_1 \log \mu_3 + \beta_1 \lambda(y) + \beta_2 \kappa(b) \tag{24}$$

with $\alpha_1 + \alpha_2 = 1$, $\beta_1 + \beta_2 = 1$, and $0 \leq \alpha_1, \beta_1 \leq 1$. Since $\alpha_1 = 0$ if and only if $\beta_1 = 0$, this is a maximum if either $\alpha_1 = \beta_1 = 0$, or $\alpha_1 = \beta_1 = 1$. This shows that, for fixed values of (h_0, a, b, y) , there exists an M such that for all $m > M$,

$$\frac{1}{m} \log S_{m,m}^{\alpha_2\alpha_1\beta_1\beta_2}(h_0; a, b, y) \leq \max(\kappa(a) + \kappa(b), \lambda(y) + \log \mu_3) + 2\epsilon. \tag{25}$$

Exponentiating the above and noting that the right hand side is independent of $(\alpha_2, \alpha_1, \beta_1, \beta_2)$,

$$\max_{\alpha_1\beta_1} S_{m,m}^{\alpha_2\alpha_1\beta_1\beta_2}(h_0; a, b, y) \leq e^{m(\text{MAX} + 2\epsilon)} \tag{26}$$

where

$$\text{MAX} = \max(\kappa(a) + \kappa(b), \lambda(y) + \log \mu_3).$$

Proceed by taking logarithms of equation (22). Divide by $(2t+1)m$, and take the limit superior as $m \rightarrow \infty$ on the left hand side. Since $H = O(m)$, this gives

$$\begin{aligned} \limsup_{m \rightarrow \infty} \frac{1}{(2t+1)m} \log K^{(t)}(m, m, a, b, y) \\ \leq \limsup_{m \rightarrow \infty} \frac{t}{(2t+1)m} \log \left[\max_{\alpha_1 \beta_1} S_{m,m}^{\alpha_2 \alpha_1 \beta_1 \beta_2}(h_0; a, b, y) \right] \\ + \limsup_{m \rightarrow \infty} \frac{1}{(2t+1)m} \log \left[\max_{h_0} C_m(h_0; b, y) \right]. \end{aligned} \quad (27)$$

By equation (26),

$$\begin{aligned} \limsup_{m \rightarrow \infty} \frac{1}{(2t+1)m} \log K^{(t)}(m, m, a, b, y) \\ \leq \frac{t}{(2t+1)} (\text{MAX} + 2\epsilon) + \limsup_{m \rightarrow \infty} \frac{1}{(2t+1)m} \log \left[\max_{h_0} C_m(h_0; b, y) \right]. \end{aligned} \quad (28)$$

It remains to examine the last term above. We notice that it cannot exceed a linear combination of $\kappa(b)$ and $\lambda(y)$. Thus, if $\text{MAX} = \lambda(y) + \log \mu_3$ then $\kappa(b) \leq \lambda(y)$ and the last term is bounded by $\lambda(y)$. On the other hand, if $\text{MAX} = \kappa(a) + \kappa(b)$, then either $\kappa(b) \leq \lambda(y)$ and the last term is bounded by $\lambda(y)$, or $\kappa(b) \geq \lambda(y)$ and the last term is bounded by $\kappa(b)$. Collecting these results and taking $\epsilon \rightarrow 0^+$ gives

$$\begin{aligned} \limsup_{m \rightarrow \infty} \frac{1}{(2t+1)m} \log K^{(t)}(m_a, m_b, a, b, y) \\ \leq \frac{1}{2t+1} \max(t\kappa(a) + (t+1)\kappa(b), t\kappa(a) + t\kappa(b) + \lambda(y), (t+1)\lambda(y) + t \log \mu_3). \end{aligned}$$

This completes the case $y \geq 1$.

The case $y < 1$: If $y < 1$, then we notice that $K^{(t)}(m_a, m_b, a, b, y) < K^{(t)}(m_a, m_b, a, b, 1)$. If $y = 1$, then

$$\begin{aligned} \limsup_{m \rightarrow \infty} \frac{1}{(2t+1)m} \log K^{(t)}(m, m, a, b, 1) \\ \leq \frac{1}{2t+1} \max(t\kappa(a) + (t+1)\kappa(b), t\kappa(a) + t\kappa(b) + \log \mu_3, (2t+1) \log \mu_3). \end{aligned}$$

Evaluating the maximum gives the upper bound $(t\kappa(a) + (t+1)\kappa(b))/(2t+1)$. This completes the proof of the theorem. \square

3.2. Phase boundaries of uniform combs

3.2.1. *The case $b < b_c$:* In this case $\kappa(b) = \log \mu_3$ and

$$\zeta(a, b, y) = \max \left[\frac{t}{2t+1} \kappa(a) + \frac{t+1}{2t+1} \log \mu_3, \frac{1}{2t+1} \lambda(y) + \frac{t}{2t+1} (\kappa(a) + \log \mu_3), \frac{t+1}{2t+1} \lambda(y) + \frac{t}{2t+1} \log \mu_3 \right].$$

For $b < b_c$ and $y < 1$, $\zeta(a, b, y) = \frac{t}{2t+1} \kappa(a) + \frac{t+1}{2t+1} \log \mu_3$ which has a critical point at $a = a_c$ and there is a phase boundary from A -adsorbed to A -desorbed and no ballistic phases.

For $y > 1$, $\lambda(y) > \log \mu_3$ and $\kappa(a) \geq \log \mu_3$. For $a < a_c$, $\kappa(a) = \log \mu_3$ and the last two terms are always larger than the first. Thus for $b < b_c$, $y > 1$, $a < a_c$, $\zeta(a, b, y) = \frac{t+1}{2t+1} \lambda(y) + \frac{t}{2t+1} \log \mu_3$

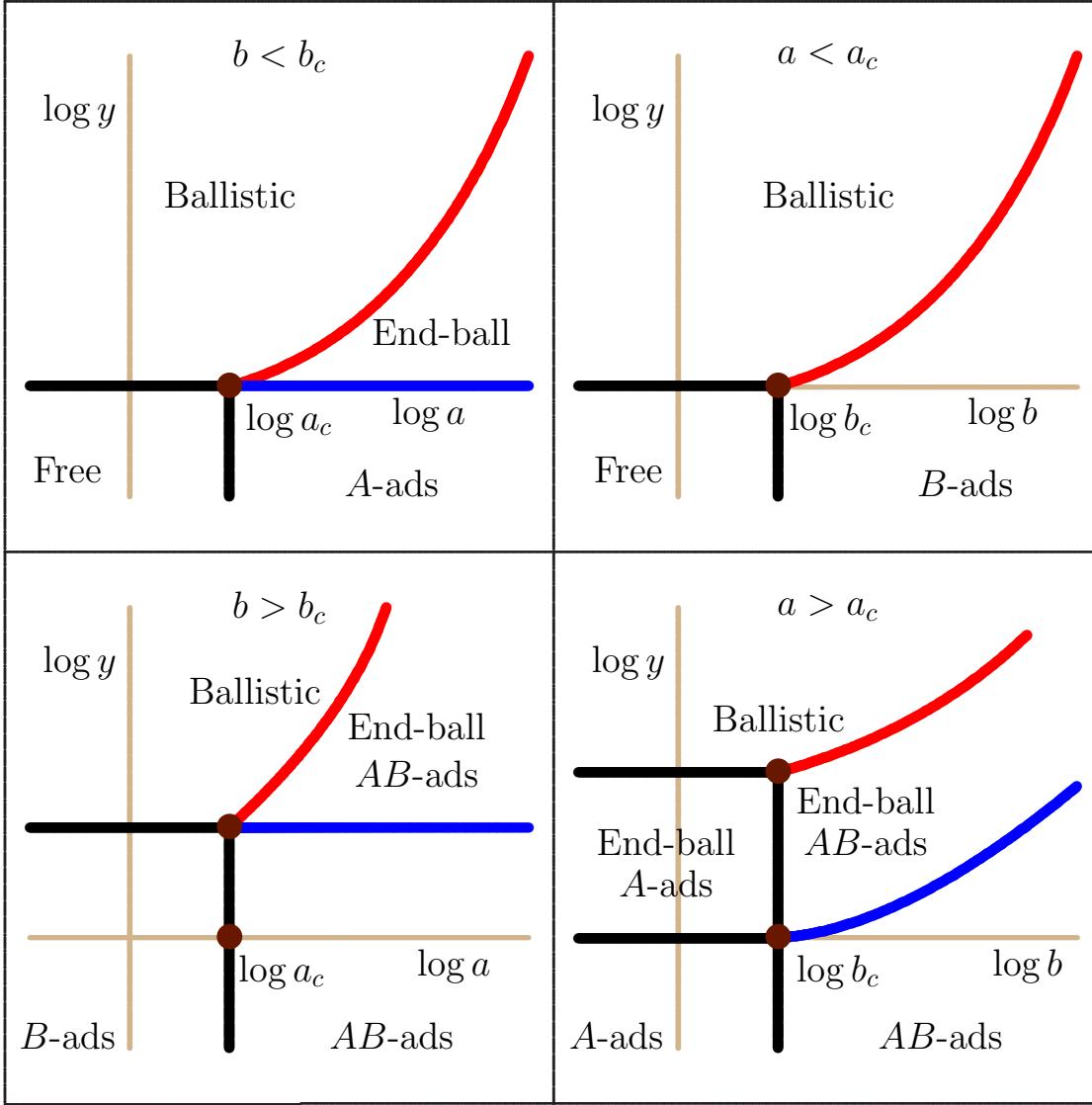


Figure 9. Phase diagrams of pulled and adsorbing uniform combs at constant a or constant b . The top left diagram is for fixed $b < b_c$ and the top right for fixed $a < a_c$. The top right diagram is qualitatively similar to that of a pulled adsorbing self-avoiding walk. On the bottom left $b > b_c$ and the backbone is adsorbed or partially adsorbed in all but the ballistic phase. The bottom right phase diagram has five phases, similar to what was established in pulled adsorbing copolymeric stars in reference [23, see figure 10(b)].

which is a fully ballistic phase. For $a > a_c$, $\kappa(a) > \log \mu_3$ and we need to compare $\lambda(y)$ and $\kappa(a)$. If $\lambda(y) < \kappa(a)$, then the middle term is larger than both the first and the last term since $\lambda(y) > \log \mu_3$.

Hence $\zeta(a, b, y) = \frac{1}{2t+1}\lambda(y) + \frac{t}{2t+1}(\kappa(a) + \log \mu_3)$ and we have an end-ballistic/ A -adsorbed phase. For $\lambda(y) > \kappa(a)$, then the last term is larger than both the first term and the middle term since $\lambda(y) > \log \mu_3$. Hence $\zeta(a, b, y) = \frac{t+1}{2t+1}\lambda(y) + \frac{t}{2t+1}\log \mu_3$ and we have a fully ballistic phase.

It follows that for $b < b_c$ and $y < 1$, there is a phase boundary from a free phase to an A -adsorbed phase at $a = a_c$ (this phase boundary is illustrated in figure 9 (top left)). If $b < b_c$ and $y > 1$, there is a phase boundary at $\lambda(y) = \kappa(a)$ (or $y = \lambda^{-1}(\kappa(a))$) which divides a fully ballistic and an end-ballistic (and A -adsorbed) phase (the case $a < a_c$ lies in the fully ballistic phase). Along $y = 1$ and $a > a_c$ runs a phase boundary separating the A -adsorbed and end-ballistic phases. Thus the boundary $y = 1$ bounds four different phases (free, ballistic, A -adsorbed and end-ballistic); see figure 9 (top left).

The phase boundary between the ballistic and end-ballistic phases is first order, while the other phase boundaries are presumably continuous. Since $\lambda(y)$ is asymptotic to $\log y$ [18] and $\kappa(a)$ is asymptotic to $\log a + \log \mu_2$ [18, 31], the phase boundary between the ballistic and end-ballistic phases is asymptotic to $\log y = \log a + \log \mu_2$.

3.2.2. The case $a < a_c$: If $a < a_c$ then $\kappa(a) = \log \mu_3$ and

$$\zeta(a, b, y) = \max \left[\frac{t}{2t+1} \log \mu_3 + \frac{t+1}{2t+1} \kappa(b), \frac{1}{2t+1} \lambda(y) + \frac{t}{2t+1} (\kappa(b) + \log \mu_3), \frac{t+1}{2t+1} \lambda(y) + \frac{t}{2t+1} \log \mu_3 \right].$$

The phase diagram of this case is illustrated in figure 9 (top right).

For $y < 1$, $\lambda(y) = \log \mu_3$ and $\kappa(b) \geq \log \mu_3$ thus the first term is always greater than the other two. Thus for $a < a_c$ and $y < 1$, the free energy $\zeta(a, b, y) = \frac{t+1}{2t+1} \kappa(b) + \frac{t}{2t+1} \log \mu_3$ which has a critical point at $b = b_c$ and there is a phase boundary from B -adsorbed to B -desorbed and no ballistic phases.

For $y > 1$, $\lambda(y) > \log \mu_3$ and $\kappa(b) \geq \log \mu_3$. For $b < b_c$, $\kappa(b) = \log \mu_3$ and the last term is always larger than the other two. Thus for $a < a_c$, $y > 1$, $b < b_c$, the free energy $\zeta(a, b, y) = \frac{t+1}{2t+1} \lambda(y) + \frac{t}{2t+1} \log \mu_3$ which is a fully ballistic phase. For $b > b_c$, $\kappa(b) > \log \mu_3$ and we need to compare $\lambda(y)$ and $\kappa(b)$. If $\lambda(y) < \kappa(b)$, then the first term is greater than the other two since $\lambda(y) > \log \mu_3$. Hence $\zeta(a, b, y) = \frac{t}{2t+1} \log \mu_3 + \frac{t+1}{2t+1} \kappa(b)$ which corresponds to a B -adsorbed/tooth-free phase (not end ballistic). For $\lambda(y) > \kappa(b)$, then the last term is greater than both the first term and the middle term since $\lambda(y) > \log \mu_3$. Hence $\zeta(a, b, y) = \frac{t+1}{2t+1} \lambda(y) + \frac{t}{2t+1} \log \mu_3$ and we have a fully ballistic phase.

Thus for $a < a_c$ and $y < 1$, there is a phase boundary from a free phase to a B -adsorbed phase at $b = b_c$.

For $y > 1$, there is a phase boundary at $\lambda(y) = \kappa(b)$ ($y = \lambda^{-1}(\kappa(b))$) which divides a ballistic phase for large y from the B -adsorbed phase at large b (the region $b < b_c$ and $y > 1$ is in the fully ballistic phase). There is no end-ballistic phase in this phase diagram. At the point $b = b_c$ and $y = 1$ there are three phase boundaries meeting, as shown in figure 9 (top right).

The phase boundary between the ballistic and B -adsorbed phases is first order, while the other phase boundaries are presumably continuous. The phase boundary between the ballistic and B -adsorbed phases is asymptotic to $\log y = \log b + \log \mu_2$.

3.2.3. The case $b > b_c$: The phase diagram is illustrated in figure 9 (bottom left). If $b > b_c$ then $\kappa(b) > \log \mu_3$. In the case that $a < a_c$, then, as discussed above, for $y < 1$ or $y > 1$ and $\lambda(y) < \kappa(b)$, the free energy $\zeta(a, b, y) = \frac{t+1}{2t+1} \kappa(b) + \frac{t}{2t+1} \log \mu_3$ which corresponds to a B -adsorbed/tooth-free

phase, while for $y > 1$ and $\lambda(y) > \kappa(b)$, the free energy $\zeta(a, b, y) = \frac{t+1}{2t+1}\lambda(y) + \frac{t}{2t+1}\log \mu_3$ and we have a fully ballistic phase.

If $a > a_c$, $\kappa(a) > \log \mu_3$, and if $y < 1$, then $\lambda(y) = \log \mu_3$ and the first term is larger than the other two so that $\zeta(a, b, y) = \frac{t}{2t+1}\kappa(a) + \frac{t+1}{2t+1}\kappa(b)$ which corresponds to an AB -adsorbed phase. If $y > 1$, we need to compare all three terms. We get three potential boundaries, namely: (1) $\lambda(y) = \kappa(b)$ (when the first two terms are equal; these terms are larger than the third term since $\kappa(a) > \log \mu_3$); (2) $\lambda(y) = \frac{t}{t+1}(\kappa(a) - \log \mu_3) + \kappa(b)$ (when the first and last terms are equal, the middle term is the maximum); (3) lastly, $\lambda(y) = (\kappa(a) - \log \mu_3) + \kappa(b)$ (the last two terms are equal; these terms are larger than the first term since $\lambda(y) > \kappa(b)$).

Thus, when $a > a_c$ and $y > 1$ there are three regions. These are $\lambda(y) < \kappa(b)$ where the free energy is given by the first term and we have an AB -adsorbed phase; $\kappa(b) < \lambda(y) < (\kappa(a) - \log \mu_3) + \kappa(b)$ where the free energy is given by the middle term and we have an end-ballistic phase; $\lambda(y) > (\kappa(a) - \log \mu_3) + \kappa(b)$ where the free energy is given by the last term and we have a fully ballistic phase.

There are four phases (namely B -adsorbed, AB -adsorbed, ballistic and end-ballistic) meeting at a multicritical point located at $\lambda(y) = \kappa(b)$ and $a = a_c$. The phase boundary $y = \lambda^{-1}(\kappa(b))$ separates the B -adsorbed and ballistic phases when $a < a_c$, and the AB -adsorbed and end-ballistic phases when $a > a_c$. The phase boundary between the B -adsorbed and AB -adsorbed phases is $a = a_c$, and the phase boundary between the ballistic and end-ballistic phases is $\lambda(y) = (\kappa(a) - \log \mu_3) + \kappa(b)$.

The phase boundary between the ballistic and end-ballistic phases is first order, but the other phase boundaries are presumably continuous. The phase boundary between the ballistic and end-ballistic phases is asymptotic to $\log y = \log a + \log b + 2 \log \mu_2 - \log \mu_3$.

3.2.4. The case $a > a_c$: The phase diagram is illustrated in figure 9 (bottom right). Since $a > a_c$, $\kappa(a) > \log \mu_3$.

If $b < b_c$ and $y < 1$ then $\zeta(a, b, y) = \frac{t}{2t+1}\kappa(a) + \frac{t+1}{2t+1}\log \mu_3$ which corresponds to an A -adsorbed phase.

If $b < b_c$ and $y > 1$, then for $\lambda(y) < \kappa(a)$, the free energy $\zeta(a, b, y) = \frac{1}{2t+1}\lambda(y) + \frac{t}{2t+1}(\kappa(a) + \log \mu_3)$ and we have an end-ballistic/ A -adsorbed phase. For $\lambda(y) > \kappa(a)$, the free energy $\zeta(a, b, y) = \frac{t+1}{2t+1}\lambda(y) + \frac{t}{2t+1}\log \mu_3$ and we have a ballistic phase.

These phases for $b < b_c$ are shown as “ A -adsorbed”, “end-ballistic”, and “ballistic” in figure 9 (bottom right).

The case $b > b_c$ and $y < 1$ gives $\zeta(a, b, y) = \frac{t}{2t+1}\kappa(a) + \frac{t+1}{2t+1}\kappa(b)$ which corresponds to an AB -adsorbed phase.

If $y > 1$ and $b > b_c$, we have three phases: (1) If $\lambda(y) < \kappa(b)$ then the free energy is given by the first term and we have an AB -adsorbed phase; (2) if $\kappa(b) < \lambda(y) < (\kappa(a) - \log \mu_3) + \kappa(b)$ then the free energy is given by the middle term and we have an end-ballistic/ AB -adsorbed phase; (3) if $\lambda(y) > (\kappa(a) - \log \mu_3) + \kappa(b)$ where the free energy is given by the last term and we have a ballistic phase.

These phases for $b > b_c$ are shown as “ballistic”, “end-ballistic/ AB -adsorbed”, and “ AB -adsorbed” in figure 9 (bottom right).

The phase boundary between the ballistic and end-ballistic phases is asymptotic to $\log y = \log b + \log a + 2 \log \mu_2 - \log \mu_3$, and the phase boundary between the end-ballistic and AB -adsorbed

phases is asymptotic to $\log y = \log b + \log \mu_2$. Notice that these curves are parallel in the $(\log y)$ - $(\log b)$ plane.

3.2.5. The (a, b) -plane for $y > 1$: In figure 10 we show a slice through the three dimensional phase diagram at fixed $y > 1$. At small values of a and b the system is ballistic. If b increases at fixed $a < a_c$ we enter a phase where the backbone is adsorbed for $b > b^*$, where $b^* = \kappa^{-1}(\lambda(y))$. (The inverse function exists since $\kappa(b)$ is continuous and strictly monotone for $b > b_c$ [7].) If a increases at fixed $b < b_c$ the teeth adsorb when $a > a^*$ where $a^* = \kappa^{-1}(\lambda(y))$. In this phase the last branch of the backbone is ballistic and the teeth are adsorbed. If $a > a_c$ and $b > b^*$ the backbone and the teeth are adsorbed and we have an AB -adsorbed phase. There is also a curved phase boundary between the ballistic phase and a phase in which the teeth are adsorbed, all except the last branch of the backbone are adsorbed, and the last branch is ballistic. This boundary is given by the solution of the equation $\lambda(y) + \log \mu_3 = \kappa(a) + \kappa(b)$, and the boundary is concave down in the $(\log a, \log b)$ -plane. To see this, take two points on the phase boundary, say $(\log a_1, \log b_1)$ and $(\log a_2, \log b_2)$. The free energy is equal to $((t+1)\lambda(y) + t \log \mu_3)/(2t+1)$ at both these points. Since the free energy is a convex function, the free energy is less than or equal to $((t+1)\lambda(y) + t \log \mu_3)/(2t+1)$ at the mid-point of the chord joining these points, so that this point is on or below the phase boundary. The concavity of the boundary then follows from the mid-point theorem.

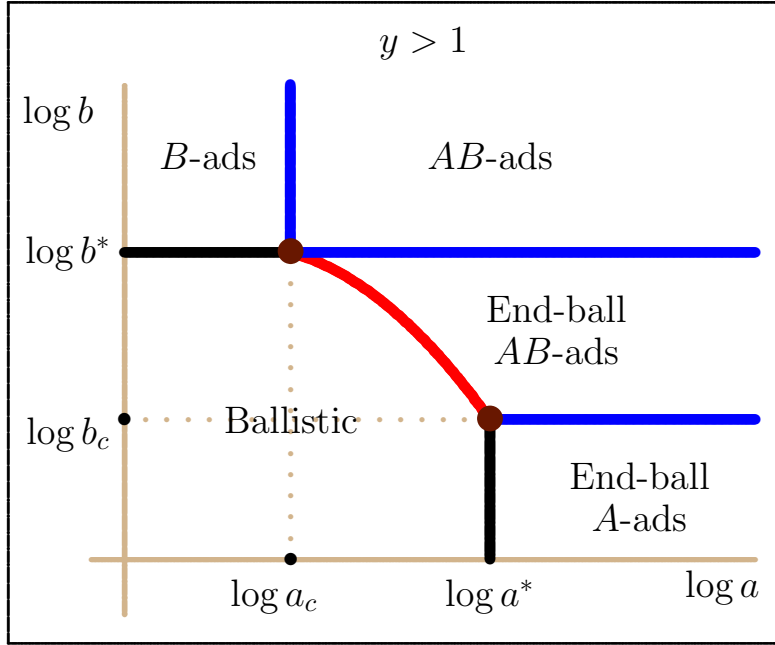


Figure 10. Phase diagram in the $(\log a, \log b)$ -plane for fixed $y > 1$. Here, $a^* = \kappa^{-1}(\lambda(y))$ and $b^* = \kappa^{-1}(\lambda(y))$. The curved phase boundary is given by the solution of $\kappa(b) = \lambda(y) - \kappa(a) + \log \mu_3$ and is concave down.

4. Non-uniform combs

In this section we examine the limits that the teeth are short compared to the backbone, or the backbone is short compared to the teeth.

4.1. Short teeth and long backbone

As before, the number of teeth is fixed at t and we are considering combs with initial vertex at the origin, in the half-space $x_3 \geq 0$, with m_a edges in each tooth, m_b edges in each segment of the backbone, v_A A -visits, v_B B -visits and having the terminal vertex at height h , and with partition function:

$$K^{(t)}(m_a, m_b, a, b, y) = \sum_{v_A, v_B, h} k^{(t)}(m_a, m_b, v_A, v_B, h) a^{v_A} b^{v_B} y^h. \quad (29)$$

With t and m_a fixed, we have the following lemma as $m_b \rightarrow \infty$:

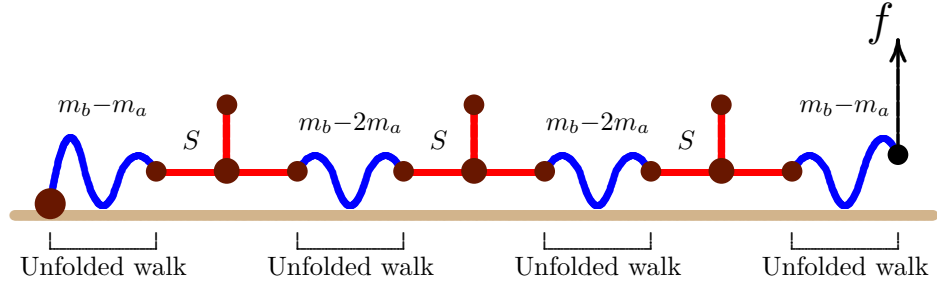


Figure 11. Concatenating unfolded walks with the structure S recursively to form a pulled adsorbing comb. The branches along the backbone each have length m_b and the straight teeth are each of length m_a . Each of the three branches of the structure S has length m_a .

Lemma 5. If t and m_a are both fixed, with the total number of edges in the comb being given by $n = (t + 1)m_b + tm_a$, the free energy is given by

$$\lim_{m_b \rightarrow \infty} \frac{1}{(t+1)m_b + tm_a} \log K^{(t)}(m_a, m_b, a, b, y) = \max[\kappa(b), \lambda(y)] = \psi(b, y).$$

Proof: Define a structure S to be $2m_a$ edges in the x_1 -direction and m_a edges starting at the centre vertex of this subwalk and extending in the x_3 -direction. This is a 3-star with m_a edges in each arm, and each arm being a straight line. Construct a comb with t teeth, each tooth with m_a edges, and a backbone of total length $(t + 1)m_b$, as follows (see figure 11). Take a walk unfolded in the x_1 -direction of length $m_b - m_a$, concatenated with a structure S , then recursively concatenated with a walk unfolded in the x_1 -direction of length $m_b - 2m_a$, concatenated with an S , a total of t times, and ending with a walk unfolded in the x_1 -direction of length $m_b - m_a$.

Consider the subset of these combs with the first s nodes of degree 3 in $x_3 = 0$ plane (that is, the first s x_1 -unfolded walks are loops) and the remaining $t - s$ nodes of degree 3 located in the half-space $x_3 > 0$. If $s = 0$ this gives the lower bound

$$\log K^{(t)}(m_a, m_b, a, b, y) \geq (m_b - m_a)\psi(b, y) + ((t - 1)(m_b - 2m_a)\lambda(y) + (m_b - m_a)\lambda(y) + o(m_b)).$$

If $s = t$ then the lower bound

$$\log K^{(t)}(m_a, m_b, a, b, y) \geq (m_b - m_a)\kappa(b) + 2tm_a \log b + (t-1)(m_b - 2m_a)\kappa(b) + (m_b - m_a)\psi(b, y) + o(m_b)$$

is obtained instead. Also, if $0 < s < t$ we have the lower bound

$$\begin{aligned} \log K^{(t)}(m_a, m_b, a, b, y) &\geq (m_b - m_a)\kappa(b) + 2sm_a \log b + (s-1)(m_b - 2m_a)\kappa(b) \\ &\quad + (m_b - 2m_a)\psi(b, y) + (t-s-1)(m_b - 2m_a)\lambda(y) \\ &\quad + (m_b - m_a)\lambda(y) + o(m_b). \end{aligned}$$

Since s is arbitrary we can choose its value to optimize the bound. When $\kappa(b) > \lambda(y)$ the bound is most effective when $s = t$ and when $\lambda(y) > \kappa(b)$ it is most effective when $s = 0$. Dividing by $(t+1)m_b + tm_a$ and letting $m_b \rightarrow \infty$ with t and m_a fixed gives

$$\liminf_{m_b \rightarrow \infty} \frac{1}{(t+1)m_b + tm_a} \log K^{(t)}(m_a, m_b, a, b, y) \geq \max[\kappa(b), \lambda(y)] = \psi(b, y).$$

To obtain an upper bound we can regard the comb as being composed of a backbone with $(t+1)m_b$ edges and t teeth, and treat these components as being independent. This gives the bound

$$\log K^{(t)}(m_a, m_b, a, b, y) \leq (t+1)m_b\psi(b, y) + tm_a\kappa(a) + o(m_b).$$

Dividing by $(t+1)m_b + tm_a$ and letting $m_b \rightarrow \infty$ with t and m_a fixed gives

$$\limsup_{m_b \rightarrow \infty} \frac{1}{(t+1)m_b + tm_a} \log K^{(t)}(m_a, m_b, a, b, y) \leq \psi(b, y).$$

This completes the proof. \square

This can be extended to the situation where t is fixed and m_b goes to infinity with $m_a = o(m_b)$. We give this result in the next theorem.

Theorem 2. *If t is fixed and m_b goes to infinity with $m_a = o(m_b)$ the free energy is given by*

$$\lim_{m_b \rightarrow \infty, m_a = o(m_b)} \frac{1}{(t+1)m_b + tm_a} \log K^{(t)}(m_a, m_b, a, b, y) = \max[\kappa(b), \lambda(y)] = \psi(b, y).$$

Proof: Since m_a being fixed is a special case of $m_a = o(m_b)$ the result of the previous lemma gives the lower bound

$$\liminf_{m_b \rightarrow \infty, m_a = o(m_b)} \frac{1}{(t+1)m_b + tm_a} \log K^{(t)}(m_a, m_b, a, b, y) \geq \psi(b, y).$$

We can obtain an upper bound by considering the case where the backbone and teeth behave independently. Again we have

$$\log K^{(t)}(m_a, m_b, a, b, y) \leq (t+1)m_b\psi(b, y) + tm_a\kappa(a) + o(m_b).$$

Dividing by $(t+1)m_b + tm_a$ and letting $m_b \rightarrow \infty$ with t fixed and $m_a = o(m_b)$ gives

$$\limsup_{m_b \rightarrow \infty, m_a = o(m_b)} \frac{1}{(t+1)m_b + tm_a} \log K^{(t)}(m_a, m_b, a, b, y) \leq \psi(b, y),$$

which completes the proof. \square

This result is expected, since the backbone dominates the partition function in the limit; this is the walk limit in this model.

4.2. Long teeth and short backbone

Assume that t is fixed, $m_b = o(m_a)$ and that if the limit $m_a \rightarrow \infty$ is taken, then $m_b \rightarrow \infty$ as well. In this case the teeth are long while the backbone is short, and the partition function is again given by equation (29). An upper bound is found by considering the teeth to be self-avoiding walks independent of one another and of the backbone. Denoting the partition function of pulled adsorbing positive walks by $C_n^+(b, y)$ (see equation (4)), and the partition function of adsorbing self-avoiding walks by $C_n(a)$, this shows that

$$\begin{aligned} & \limsup_{m_a \rightarrow \infty} \frac{1}{t m_a + (t+1) o(m_a)} \log K^{(t)}(m_a, o(m_a), a, b, y) \\ & \leq \limsup_{m_a \rightarrow \infty} \frac{1}{t m_a + (t+1) o(m_a)} \left((t+1) \log C_{o(m_a)}^+(b, y) + t \log C_{m_a}(a) \right) = \kappa(a). \end{aligned} \quad (30)$$

For a lower bound, equation (16) holds here and gives

$$K^{(t)}(m_a, m_b, a, b, y) \geq \left[L_{o(m_a)}^{\dagger[1]}(>w, b) \right]^t \left[L_{o(m_a)}^{\dagger[1]}(b) \right]^1 \left[C_{m_a-u}^{(w)}(a) \right]^t. \quad (31)$$

Take logarithms, divide by $t m_a + (t+1) o(m_a)$, and then take $m_a \rightarrow \infty$. By lemma 2,

$$\liminf_{m_a \rightarrow \infty} \frac{1}{t m_a + (t+1) o(m_a)} \log K^{(t)}(m_a, o(m_a), a, b, y) \geq \kappa^{(w)}(a). \quad (32)$$

Since w is arbitrary, one may take $w \rightarrow \infty$ on the right hand side. By lemma 2, $\kappa^{(w)}(a) \rightarrow \kappa(a)$, and comparing this result to equation (30), the following theorem is obtained.

Theorem 3. $\lim_{m_a \rightarrow \infty} \frac{1}{t m_a + (t+1) o(m_a)} \log K^{(t)}(m_a, o(m_a), a, b, y) = \kappa(a).$ \square

This result is expected, since the adsorbing teeth dominate the partition function in the limit. Since the backbone has length $o(m_a)$, the pulling force cannot pull any teeth from the adsorbing plane, and if the teeth are adsorbed, then so is the backbone. This is the star limit in this model.

5. The limit t approaches infinity

In this section the limit as $t \rightarrow \infty$ is examined. In this limit the comb becomes of infinite length, but with the lengths of teeth and of the segments between teeth, fixed at m_a and m_b respectively.

Denote by $g(m_a, m_b, t)$ the number of combs from the origin, in the bulk lattice \mathbb{Z}^3 , with t teeth of length m_a and $t+1$ backbone segments of length m_b . Then a comb from the origin of backbone length equal to $(s+t)m_b$ with $s+t-1$ teeth of length m_a , can be cut, at the node along the backbone where the s -th tooth is attached, into two subcombs with $s-1$ teeth and $t-1$ teeth respectively, and a tooth which is a self-avoiding walk of length m_a . This shows that

$$g(m_a, m_b, s+t-1) \leq c_{m_a} g(m_a, m_b, s-1) g(m_a, m_b, t-1), \quad (33)$$

where c_{m_a} accounts for the conformations of the orphaned tooth and is the number of self-avoiding walks of length m_a from the origin in the lattice. This shows that $c_{m_a} g(m_a, m_b, t)$ satisfies a submultiplicative inequality, and by reference [11] the connective constant [6] of lattice combs is defined by

$$\zeta_{m_a, m_b} = \lim_{t \rightarrow \infty} \frac{1}{t} \log g(m_a, m_b, t) = \inf_{t \geq 0} \frac{1}{t} \log (c_{m_a} g(m_a, m_b, t)). \quad (34)$$

Notice that $\zeta_{0, m_b} = m_b \log \mu_3$ where μ_3 is the growth constant of the self-avoiding walk.

5.1. Grafted combs pulled at an endpoint

In this section we consider models of adsorbing combs in the half-lattice where, as above, the backbone of the comb is taken to infinity by letting $t \rightarrow \infty$ (but with (m_a, m_b) fixed).

For a lower bound, equation (19) holds here for $y \geq 1$, that is for $w < h_y$ and $a, b \geq 0$:

$$K^{(t)}(m_a, m_b, a, b, y) \geq K^{(t)}(m_a, m_b, 0, 0, y) \geq \left[\ell_{m_b}^{\dagger[3]}(h_y) y^{h_y} \right]^{t+1} \left[c_{m_a-u}^{\dagger[1],(w)} \right]^t, \quad (35)$$

where $K^{(t)}(m_a, m_b, 0, 0, y)$ denotes the partition function for combs with the backbone and the teeth disjoint from the adsorbing surface (except at the origin).

Take logarithms, divide by $(t+1)m_b + tm_a$ and let $t \rightarrow \infty$:

$$\begin{aligned} & \frac{1}{m_b + m_a} \log \left[\ell_{m_b}^{\dagger[3]}(h_y) y^{h_y} \right] + \frac{1}{m_b + m_a} \log c_{m_a-u}^{\dagger[1],(w)} \\ & \leq \liminf_{t \rightarrow \infty} \frac{1}{(t+1)m_b + tm_a} \log K^{(t)}(m_a, m_b, 0, 0, y) = \Lambda_{inf}(m_a, m_b, 0, 0, y). \end{aligned} \quad (36)$$

To find an upper bound, use a construction similar to figure 6. Replace the backbone with a positive self-avoiding walk of length $(t+1)m_b$ from the origin, and pulled at its endpoint. The teeth are replaced by self-avoiding walks, each of length $m_a - u$. This gives

$$K^{(t)}(m_a, m_b, 1, 1, y) \leq C_{(t+1)m_b}^+(1, y) [c_{m_a-u}]^t. \quad (37)$$

Take logarithms, divide by $(t+1)m_b + tm_a$ and let $t \rightarrow \infty$:

$$\begin{aligned} \Lambda_{sup}(m_a, m_b, 1, 1, y) &= \limsup_{t \rightarrow \infty} \frac{1}{(t+1)m_b + tm_a} \log K^{(t)}(m_a, m_b, 1, 1, y) \\ &\leq \frac{m_b}{m_b + m_a} \lambda(y) + \frac{1}{m_b + m_a} \log c_{m_a-u}. \end{aligned} \quad (38)$$

The bounds in equations (36) and (38) are valid in the square and in the cubic lattices.

The bounds above are independent of a and b , but may be generalised by noting that for $0 \leq a, b \leq 1$ and $y \geq 1$,

$$K^{(t)}(m_a, m_b, 0, 0, y) \leq K^{(t)}(m_a, m_b, a, b, y) \leq K^{(t)}(m_a, m_b, 1, 1, y). \quad (39)$$

5.2. Adsorbed pulled combs

In this section consider a fully adsorbed comb grafted at its first vertex, and being pulled at its endpoint by a vertical force.

For a lower bound, equation (16) holds here and gives

$$K^{(t)}(m_a, m_b, a, b, y) \geq \left[L_{m_b}^{\dagger[1]}(>w, b) \right]^t \left[L_{m_b}^{\dagger[1]}(b) \right]^1 \left[C_{m_a-u}^{(w)}(a) \right]^t. \quad (40)$$

Taking logarithms, dividing by $(t+1)m_b + tm_a$ and then taking $t \rightarrow \infty$ gives for any choice of w ,

$$\begin{aligned} & \frac{1}{m_b + m_a} \log L_{m_b}^{\dagger[1]}(>w, b) + \frac{1}{m_b + m_a} \log C_{m_a-u}^{(w)}(a) \\ & \leq \liminf_{t \rightarrow \infty} \frac{1}{(t+1)m_b + tm_a} \log K^{(t)}(m_a, m_b, a, b, y) = \Lambda_{inf}(m_a, m_b, a, b, y). \end{aligned} \quad (41)$$

An upper bound is obtained by replacing the loops and walks in figure 5 with adsorbing positive self-avoiding walks. This shows that, for $a, b \geq 0$ and $y \geq 0$,

$$\begin{aligned} \Lambda_{sup}(m_a, m_b, a, b, y) &= \limsup_{t \rightarrow \infty} \frac{1}{(t+1)m_b + tm_a} \log K^{(t)}(m_a, m_b, a, b, y) \\ &\leq \frac{1}{m_b + m_a} \log C_{m_b}^+(b) + \frac{1}{m_b + m_a} \log C_{m_a}^+(a), \end{aligned} \quad (42)$$

where $C_n^+(a)$ is the partition function of adsorbing positive walks. These bounds are valid in the cubic lattice.

5.3. Limits in the cubic lattice

The limit $t \rightarrow \infty$ is an infinite comb with finite segments of length m_b along the backbone, and teeth each of finite length m_a . If $m_a \rightarrow \infty$ with $m_b = o(m_a)$ and diverging, then the limiting object will be a star with an infinite number of arms (this will be the *star limit*), and, if instead, $m_b \rightarrow \infty$ with $m_a = o(m_b)$ and diverging, then the limit should be a *self-avoiding walk limit*.

One may also calculate limits of intermediate combs by putting $m_b = \lfloor \alpha n \rfloor$ and $m_a = \lfloor (1 - \alpha)n \rfloor$ and then taking $n \rightarrow \infty$. These limits are given in the following theorems.

Consider the star limit first.

Theorem 4 (Star limit). *If $m_a \rightarrow \infty$ and $m_b = o(m_a)$ and divergent, the free energy is given by*

$$\Lambda(a, b, y) = \lim_{m_a \rightarrow \infty} \Lambda_{inf}(m_a, o(m_a), a, b, y) = \lim_{m_a \rightarrow \infty} \Lambda_{sup}(m_a, o(m_a), a, b, y) = \kappa(a)$$

for all $a, b \geq 0$ and $y > 0$.

Proof. By equation (36) a lower bound on the free energy in the limit as $m_a \rightarrow \infty$ (and $m_b = o(m_a)$) is, for all $y > 0$ and $a, b \geq 0$,

$$\liminf_{m_a \rightarrow \infty} \Lambda_{inf}(m_a, o(m_a), a, b, y) \geq \liminf_{m_a \rightarrow \infty} \Lambda_{inf}(m_a, o(m_a), 0, 0, y) = \log \mu_3 = \kappa(1).$$

Notice that there is no dependence on y .

Similarly, by equation (41) for $y > 0$ and $a, b \geq 0$,

$$\liminf_{m_a \rightarrow \infty} \Lambda_{inf}(m_a, o(m_a), a, b, y) \geq \kappa^{(w)}(a).$$

If $m_a \rightarrow \infty$, and $w \leq m_b = o(m_a) \rightarrow \infty$, it follows that w can be increased without bound. Since $\kappa^{(w)}(a) \rightarrow \kappa(a)$ by lemma 2, this shows that for all $y > 0$, and $a, b \geq 0$,

$$\liminf_{m_a \rightarrow \infty} \Lambda_{inf}(m_a, o(m_a), a, b, y) \geq \kappa(a).$$

Next, taking $m_a \rightarrow \infty$ with $m_b = o(m_a) \rightarrow \infty$, it follows from equation (38) that for $y \geq 0$ and $a \geq 0$,

$$\limsup_{m_a \rightarrow \infty} \Lambda_{sup}(m_a, o(m_a), 1, 1, y) \leq \kappa(a).$$

By equation (42)

$$\limsup_{m_a \rightarrow \infty} \Lambda_{sup}(m_a, o(m_a), a, b, y) \leq \kappa(a)$$

for all $y \geq 0$ and $a, b \geq 0$.

Comparing the upper and lower bounds establishes that, for $y > 0$ and $a, b \geq 0$,

$$\lim_{m_a \rightarrow \infty} \Lambda_{inf}(m_a, o(m_a), a, b, y) = \lim_{m_a \rightarrow \infty} \Lambda_{sup}(m_a, o(m_a), a, b, y) = \kappa(a),$$

by equations (36), (38), (41) and (42). This completes the proof. \square

The star limit in theorem 4 shows that there is a critical plane $a = a_c$ in the *aby*-phase diagram where the star adsorbs. There is no ballistic phase for any finite $y \geq 0$, so that the star cannot be pulled from the adsorbing plane. The node of the star is the limit of the backbone of the comb, and since the backbone is both grafted to the adsorbing surface, and pulled by the vertical force, it cannot be pulled from the adsorbing surface.

Next, consider the limits when $m_b = \lfloor \alpha n \rfloor$ and $m_a = \lfloor (1 - \alpha)n \rfloor$ for an $\alpha \in (0, 1)$. Then taking $n \rightarrow \infty$ also take m_b and m_a to infinity. By equations (36) and (41),

$$\liminf_{n \rightarrow \infty} \Lambda_{inf}(\lfloor \alpha n \rfloor, \lfloor (1 - \alpha)n \rfloor, a, b, y) \geq \begin{cases} \alpha \kappa(b) + (1 - \alpha) \kappa^{(w)}(a) \\ \alpha \lambda(y) + (1 - \alpha) \log \mu^{(w)} \end{cases} \quad (43)$$

for all $a, b, y \geq 0$. If $y \geq 1$, then by lemma 4 the most popular width of the loops in figure 5 increases without bound as $m_b \rightarrow \infty$ in both the adsorbed and desorbed phases. Thus, the limit $w \rightarrow \infty$ can be taken on the right hand side in the above, giving

$$\liminf_{n \rightarrow \infty} \Lambda_{inf}(\lfloor \alpha n \rfloor, \lfloor (1 - \alpha)n \rfloor, a, b, y) \geq \begin{cases} \alpha \kappa(b) + (1 - \alpha) \kappa(a); \\ \alpha \lambda(y) + (1 - \alpha) \log \mu_3, \end{cases} \quad (44)$$

for $y \geq 1$ and $a, b \geq 0$.

More generally, notice that

$$K^{(t)}(\lfloor \alpha n \rfloor, \lfloor (1 - \alpha)n \rfloor, a, b, y) \geq K^{(t)}(\lfloor \alpha n \rfloor, \lfloor (1 - \alpha)n \rfloor, 0, 0, 0)$$

and that $K^{(t)}(\lfloor \alpha n \rfloor, \lfloor (1 - \alpha)n \rfloor, 0, 0, 0)$ is the number of combs from the origin to their last vertex in the plane $x_3 = 0$, and with no visits by teeth or the backbone to the plane $x_3 = 0$ otherwise. Then it follows, by using the methods of reference [34], that

$$\begin{aligned} & \liminf_{n \rightarrow \infty} \frac{1}{(t+1)\lfloor \alpha n \rfloor + t\lfloor (1-\alpha)n \rfloor} \log K^{(t)}(\lfloor \alpha n \rfloor, \lfloor (1 - \alpha)n \rfloor, a, b, y) \\ & \geq \liminf_{n \rightarrow \infty} \frac{1}{(t+1)\lfloor \alpha n \rfloor + t\lfloor (1-\alpha)n \rfloor} \log K^{(t)}(\lfloor \alpha n \rfloor, \lfloor (1 - \alpha)n \rfloor, 0, 0, 0) \\ & \geq \log \mu_3. \end{aligned} \quad (45)$$

This shows, that for every $\epsilon > 0$ there is a N_ϵ such that for all $n \geq N_\epsilon$ and $a, b, y \geq 0$,

$$K^{(t)}(\lfloor \alpha n \rfloor, \lfloor (1 - \alpha)n \rfloor, a, b, y) \geq ((t+1)\lfloor \alpha n \rfloor + t\lfloor (1 - \alpha)n \rfloor) (\log \mu_3 - \epsilon). \quad (46)$$

Thus, by the definition of $\Lambda_{inf}(\lfloor \alpha n \rfloor, \lfloor (1 - \alpha)n \rfloor, a, b, y)$ it follows that, for all $n \geq N_\epsilon$ and $a, b, y \geq 0$,

$$\begin{aligned} & \Lambda_{inf}(\lfloor \alpha n \rfloor, \lfloor (1 - \alpha)n \rfloor, a, b, y) \\ & = \liminf_{t \rightarrow \infty} \frac{1}{(t+1)\lfloor \alpha n \rfloor + t\lfloor (1-\alpha)n \rfloor} \log K^{(t)}(\lfloor \alpha n \rfloor, \lfloor (1 - \alpha)n \rfloor, a, b, y) \\ & \geq \log \mu_3 - \epsilon. \end{aligned} \quad (47)$$

Since $\epsilon > 0$ is arbitrary, it follows that for all $a, b, y \geq 0$,

$$\liminf_{n \rightarrow \infty} \Lambda_{inf}(\lfloor \alpha n \rfloor, \lfloor (1 - \alpha)n \rfloor, a, b, y) \geq \log \mu_3. \quad (48)$$

Comparing this to the right hand side of equation (44) shows that this is a lower bound for all $a, b, y \geq 0$, and hence equation (44) is valid also for all $y \geq 0$.

Theorem 5. *The limit*

$$\begin{aligned}\Lambda_\alpha(a, b, y) &= \lim_{n \rightarrow \infty} \Lambda_{sup}(\lfloor \alpha n \rfloor, \lfloor (1 - \alpha)n \rfloor, a, b, y) \\ &= \max\{\alpha \lambda(y) + (1 - \alpha) \log \mu, \alpha \kappa(b) + (1 - \alpha) \kappa(a)\}\end{aligned}$$

exists.

Proof. Consider first the case that $a, b \leq 1$. By equation (38),

$$\limsup_{n \rightarrow \infty} \Lambda_{sup}(\lfloor \alpha n \rfloor, \lfloor (1 - \alpha)n \rfloor, a, b, y) \leq \alpha \lambda(y) + (1 - \alpha) \log \mu.$$

On the other hand, if $a > a_c$, or $b > b_c$, or both, then by equation (42),

$$\limsup_{n \rightarrow \infty} \Lambda_{sup}(\lfloor \alpha n \rfloor, \lfloor (1 - \alpha)n \rfloor, a, b, y) \leq \alpha \kappa(b) + (1 - \alpha) \kappa(a).$$

These upper bounds coincide with the lower bounds in equation (44). Since these bounds are monotonic non-decreasing in each of $\{a, b, y\}$, and since $\kappa(a) = \kappa(b) = \log \mu$ for all $a \leq a_c$ and $b \leq b_c$ the result is that

$$\begin{aligned}\liminf_{n \rightarrow \infty} \Lambda_{inf}(\lfloor \alpha n \rfloor, \lfloor (1 - \alpha)n \rfloor, a, b, y) &= \limsup_{n \rightarrow \infty} \Lambda_{sup}(\lfloor \alpha n \rfloor, \lfloor (1 - \alpha)n \rfloor, a, b, y) \\ &= \max\{\alpha \lambda(y) + (1 - \alpha) \log \mu, \alpha \kappa(b) + (1 - \alpha) \kappa(a)\}.\end{aligned}$$

This completes the proof. \square

Notice that by taking $\alpha \rightarrow 0^+$ the star limit in theorem 4 is found.

The self-avoiding walk limit in the cubic lattice is encountered when $m_b \rightarrow \infty$ and $m_a = o(m_b)$ and divergent. By taking $\alpha \rightarrow 1^-$ in theorem 5, it follows that

Theorem 6 (Self-avoiding walk limit). *If $m_b \rightarrow \infty$ and $m_a = o(m_b)$ and divergent, the free energy is given by*

$$\begin{aligned}\Lambda(a, b, y) &= \lim_{m_b \rightarrow \infty} \Lambda_{inf}(o(m_b), m_b, a, b, y) \\ &= \lim_{m_b \rightarrow \infty} \Lambda_{sup}(o(m_b), m_b, a, b, y) = \max\{\kappa(b), \lambda(y)\} = \psi(b, y).\end{aligned}$$

for all $a, b \geq 0$ and $y \geq 0$. \square

6. Discussion

We have investigated a self-avoiding walk model of the adsorption of comb copolymers at a surface. These are interesting because of their use as steric stabilizers of dispersions [39]. The teeth of the comb are chemically different from the backbone of the comb and can interact differently with the surface. In addition, we have considered the effect of a force pulling the adsorbed comb off the surface. We have concentrated on the case where one end vertex of the backbone is fixed in the surface and where the force is applied at the other end of the backbone.

We have considered several cases: (i) a uniform comb where the lengths of the teeth and the backbone branches (or segments) are all equal and where the number of teeth (t) is fixed, (ii) a comb with t teeth where the teeth are short compared to the backbone branches, (iii) a comb with t teeth where the backbone branches are short compared to the teeth, and (iv) the case where the number of teeth goes to infinity. In each case we have determined the free energy rigorously and investigated the forms of the phase diagrams. In particular, for the uniform case (where the lengths

of the teeth and the backbone branches are equal and where the number of teeth is fixed) we have established the form of the phase diagram by taking various slices through the three dimensional diagram. When the teeth do not adsorb, the form of the (two dimensional) diagram is similar to that of self-avoiding walks adsorbing in a surface and being desorbed by a force [18]. When both the teeth and the backbone adsorb, there are strong similarities to the phase diagram for copolymeric stars [23].

Comparing the infinite number of teeth case (iv) to the other cases considered, our results establish that some limits can be interchanged. For case (ii), when the teeth are short compared to the backbone branches, then the walk limit is obtained whether one first lets the number of teeth (t) go to infinity and then lets the backbone length go to infinity (as in section 5.3, theorem 6) or if the limits are in the reverse order (see section 4, theorem 2). Similarly, for case (iii), when the backbone branches are short compared to the teeth, no matter the order of the limits, the star limit is obtained (see theorems 4 and 3). For the uniform case (i), comparing theorems 5 ($\alpha = 1/2$) and 1, no matter the order of the limits ($t \rightarrow \infty$, length of the branches goes to infinity) the free energy is the same. The resulting comb free energy is either equal to that of the adsorbed case ($y = 1$) or that of the pulled/non-adsorbed case ($a = b = 1$).

Although we have concentrated on the case of the simple cubic lattice our results can be extended to the d -dimensional hypercubic lattice for all $d \geq 3$, but our methods do not extend to the $d = 2$ case. The two dimensional case requires further work. In three dimensions, our methods could be extended to apply to other lattices such as the body centred and face centred cubic lattices, although we have not worked out the details.

The model can be extended in other ways, for instance to a brush copolymer where we have a backbone with t vertices of degree k and with $k - 2$ side chains (the analogue of teeth of a comb) at each of these t vertices. It would also be interesting to consider cases where the force is applied at vertices other than the terminal vertex of degree 1.

Acknowledgement

EJJvR and CES acknowledge the Natural Sciences and Engineering Research Council of Canada (NSERC) [funding reference numbers: RGPIN-2019-06303; RGPIN-2020-06339].

References

- [1] Beaton N R 2015 *J. Phys. A: Math. Theor.* **48** 16FT03
- [2] Beaton N R 2017 *J. Phys. A: Math. Theor.* **50** 494001
- [3] Bradly C J, Janse van Rensburg E J, Owczarek A L and Whittington S G 2019 *J. Phys. A: Math. Theor.* **52** 315002
- [4] Bradly C J and Owczarek A L 2019 *J. Phys. A: Math. Theor.* **52** 275001
- [5] Guttmann A J, Jensen I and Whittington S G 2014 *J. Phys. A: Math. Theor.* **47** 015004
- [6] Hammersley J M 1957 *Proc. Camb. Phil. Soc.* **53** 642-645
- [7] Hammersley J M, Torrie G and Whittington S G 1982 *J. Phys. A: Math. Gen.* **15** 539-571
- [8] Hammersley J M and Welsh D J A 1962 *Quart. J. Math. Oxford* **13** 108-110
- [9] Hammersley J M and Whittington S G 1985 *J. Phys. A: Math. Gen.* **18** 101-111
- [10] Haupt B J, Ennis J and Sevick E M 1999 *Langmuir* **15** 3886-3892
- [11] Hille E and Phillips R S 1957 *Functional Analysis and Semi-groups*, AMS
- [12] Ioffe D and Velenik Y 2008 *Ballistic phase of self-interacting random walks*, Analysis and Stochastics of Growth Processes and Interface Models (P. Morters, R. Moser, M. Penrose, H. Schwetlick, and J. Zimmer, eds.), Oxford University Press, pp. 55-79.
- [13] Ioffe D and Velenik Y 2010 *Braz. J. Prob. Stat.* **24** 279-299

- [14] Janse van Rensburg E J 1998 *J. Phys. A: Math. Gen.* **31** 8295-8306
- [15] Janse van Rensburg E J 2015 *The Statistical Mechanics of Interacting Walks, Polygons, Animals and Vesicles 2ed*, Oxford University Press, Oxford
- [16] Janse van Rensburg E J, Orlandini E, Tesi M C and Whittington S G 2009 *J. Stat. Mech.* P07014
- [17] Janse van Rensburg E J, Soteris C E and Whittington S G 2020 *J. Phys. A: Math. Theor.* **53** 505001
- [18] Janse van Rensburg E J and Whittington S G 2013 *J. Phys. A: Math. Theor.* **46** 435003
- [19] Janse van Rensburg E J and Whittington S G 2016 *J. Phys. A: Math. Theor.* **49** 11LT01
- [20] Janse van Rensburg E J and Whittington S G 2017 *J. Phys. A: Math. Theor.* **50** 055001
- [21] Janse van Rensburg E J and Whittington S G 2018 *J. Phys. A: Math. Theor.* **51** 204001
- [22] Janse van Rensburg E J and Whittington S G 2019 *J. Phys. A: Math. Theor.* **52** 115001
- [23] Janse van Rensburg E J and Whittington S G 2022 *J. Phys. A: Math. Theor.* **55** 265003
- [24] Krawczyk J, Owczarek A L, Prellberg T and Rechnitzer A 2005 *J. Stat. Mech.* P05008
- [25] Krawczyk J, Prellberg T, Owczarek A L and Rechnitzer A 2004 *J. Stat. Mech.* P10004
- [26] Madras N 2017 *J. Phys. A: Math. Theor.* **50** 064003
- [27] Madras N and Slade G 1993 *The Self-Avoiding Walk* Birkhäuser, Boston
- [28] Mishra P K, Kumar S and Singh Y 2005 *Europhys. Lett.* **69** 102-108
- [29] Napper D 1983 *Polymeric Stabilisation of Colloidal Dispersions* (New York: Academic)
- [30] Orlandini E and Whittington S G 2016 *J. Phys. A: Math. Theor.* **49** 343001
- [31] Rychlewski G and Whittington S G 2011 *J. Stat. Phys.* **145** 661-668
- [32] Skvortsov A M, Klushin L I, Fleer G J and Leermakers F A M 2009 *J. Chem. Phys.* **130** 174704
- [33] Skvortsov A M, Klushin L I, Polotsky A A and Binder K 2012 *Phys. Rev. E* **85** 031803
- [34] Soteris C E 1992 *J. Phys. A: Math. Gen.* **25** 3153-3173
- [35] Soteris C E and Whittington S G 1988 *J. Phys. A: Math. Gen.* **21** L857-L861
- [36] Whittington S G 1975 *J. Chem. Phys.* **63** 779-785
- [37] Whittington S G and Soteris C E 1991 *Israel J. Chem.* **31** 127-133
- [38] Whittington S G and Soteris C E 1992 *Macromol. Rep.* **29**(S2) 195-199
- [39] Xie G, Kryszewski P, Tilton R D and Matyjaszewski K 2017 *Macromolecules* **50** 2942-2950
- [40] Zhang W and Zhang X 2003 *Prog. Polym. Sci.* **28** 1271-1295